

Nutrient Exchange between a Salt Marsh and the Murderkill Estuary, Kent County, Delaware

Report – Part C

Dr. William Ullman^a, Dr. Anthony Aufdenkampe^b,
Dr. Rebecca L. Hays^{a,c}, and Stephanie Dix^b

^aSchool of Marine Science and Policy, University of Delaware, Lewes, DE 19958

^bStroud Water Research Center, Avondale, PA 19311

^cPresent Address: Eastern University, St. Davids, PA 19087

Report – Part C

Submitted in partial fulfillment of the reporting requirements of:

Water, Salt, and Nutrient Balances in an Estuarine Salt Marsh
(Murderkill River Estuary, Kent County, Delaware)

Project Period: 1 June 2007 to 30 November 2008

William Ullman, Anthony Aufdenkampe, Kuo-Chuin Wong

23 August 2013

Previously Submitted Reports

Report	Title	Submitted
Part A	Wong, K.-C., B. Dzwonkowski, and W.J. Ullman, 2009. On the temporal and spatial variability of sea level and volume flux in the Murderkill River estuary. <i>Estuarine, Coastal, and Shelf Science</i> 84:440-446.	9 May 2011
Part B	Dzwonkowski, B., K.-C. Wong, and W.J. Ullman, 2011. Episodic shifts in sea level and velocity characteristics of a salt marsh tidal creek of the Murderkill Estuary, DE. (now published as: Dzwonkowski, B., K.-C. Wong, and W.J. Ullman, 2013. Water level and velocity characteristics of a salt marsh channel in the Murderkill Estuary, Delaware. <i>Journal of Coastal Research</i> , doi: http://dx.doi.org/10.2112/JCOASTRES-D-12-00161.1).	9 June 2011

Table of Contents

- 1 Abstract 3**
- 2 Introduction..... 4**
 - 2.1 Study Objectives..... 4**
 - 2.2 Background: Murderkill Watershed and Estuary 4**
- 3 Approach and Methods..... 6**
 - 3.1 Sampling Site 6**
 - 3.2 Sampling Dates and Times 7**
 - 3.3 Approach..... 8**
 - 3.4 Sampling Methods..... 8**
 - 3.5 Analytical Methods..... 10**
- 4 Results and Discussion 11**
 - 4.1 Sampling Period Conditions: Normal vs. Episodic Events..... 11**
 - 4.2 Concentrations as a Function of Tidal Stage: Period MKA as an Example..... 11**
 - 4.3 Concentrations as a Function of Tidal Stage: Other Sampling Periods 18**
 - 4.4 Analysis of Loads: Failure of the Conventional Approach 26**
 - 4.5 Concentrations as a Function of Salinity: Evaluation of Conservative Mixing..... 28**
 - 4.6 Analysis of Loads: Novel Approach Using Anomalies to Conservative Mixing 33**
 - 4.7 Recommended oxidation ratios for the respiration of organic matter..... 38**
 - 4.8 Implications for the Murderkill Estuary..... 40**
- 5 Acknowledgements:..... 41**
- 6 Citations 42**
- 7 Appendices: 45**

Nutrient Exchange Between a Salt Marsh and the Murderkill Estuary, Kent County Delaware. Part C.

Dr. William Ullman, Dr. Anthony Aufdenkampe,
Dr. Rebecca L. Hays, and Stephanie Dix

1 Abstract

Based on extensive sampling of one polyhaline salt marsh (Webbs Marsh) that discharges to the Murderkill Estuary, salt marshes in this system can be both sinks and sources of biogeochemically reactive dissolved and particulate species. Loads are clearly variable on hourly time scales due to tidal exchange. However, on longer time scales both astronomical and wind driven tidal effects and seasonal patterns of biogeochemical processes are important controls on exchange rates. As a consequence, exchange rates of these substances are extremely variable and repeatable patterns on time scales longer than a day are difficult to impossible to discern and predict. Much of the water that enters the marsh from the main stem of the Murderkill Estuary exits with little change in its composition and, due to the relatively high mixing rates and turbidity characteristic of this estuary, retains the conservative distribution patterns observed in the Estuary. Only a small number of samples from each tidal cycle show evidence of addition to or removal from the Murderkill Estuarine waters. A novel approach for estimating marsh exchange rates, based on the extent and persistence of deviation from observed conservation in the ebb-tidal waters, was used to quantify nutrient, carbon, particle, and oxygen exchange between the Murderkill and Webbs Marsh for ~40 hour periods, on five occasions, during 2007 and 2008 (July 2007; October 2007; April 2008; May 2008; August 2008). This method is less sensitive to water imbalance and reduces the propagation of uncertainties to a greater extent than traditional hourly summation techniques. Processes contributing to nutrient, carbon, and particle loads include lateral exchange between marsh pore waters and tidal channels during flood and ebb tides (in between which oxidized species are reduced and reduced species are released to interstitial and marsh waters) and erosion and resuspension of detrital particles in the marshes and in marsh channels. For most species determined and on most dates, the net flux of biogeochemically reactive species was from the marsh to the Estuary and ultimately to Delaware Bay. Exceptions include nitrate and dissolved oxygen – oxidized species that are reduced in the marsh – for which net fluxes were into the marsh on all but one occasion. Also, during April 2008, net fluxes of many species were also toward the marsh. Based on C/N ratios and the stable isotopic compositions of particles ($\delta^{13}\text{C}$ and $\delta^{15}\text{N}$), there are two distinct sources of organic matter in the Murderkill Estuary and associated marshes; fine particles have compositions consistent with phytoplankton and soil organic matter sources and coarse particles and dissolved organic matter have compositions consistent with a vascular plant (including marsh plants) source. Dissolved and particulate organic matter and NH_4^+ released from marshes to the Murderkill Estuary all contribute significantly, albeit variably, to oxygen demand in the Estuary. However, the oxygen deficit (the amount of O_2 necessary to bring watermasses back to saturation) is also significant during most sampling periods, sometimes representing approximately half of the total exported biogeochemical oxygen demand. The oxygen deficit load from the marsh has immediate

impacts on O₂ concentration in the Murderkill Estuary and could be responsible for some or all of the observed hypoxia and onset of hypoxia in this system.

2 Introduction

2.1 Study Objectives

The **principal objective** of this project was to determine whether the salt marshes that abut and drain to the Murderkill Estuary represent significant sources or sinks of nutrients, carbon, and oxygen demand to the Estuary. This objective was addressed by determining the concentrations of dissolved oxygen and dissolved and particulate carbon, nitrogen and phosphorus species in the tidal channel connecting one polyhaline salt marsh (Webbs Marsh) to the Estuary together with discharge and other continuous data collected at the same station ([USGS Station 01484084](#), Unnamed Ditch near Webb Landing at South Bowers, DE, [39.050333°N, -75.391306°W](#)). This particular salt marsh was selected because: (1) it has no significant upland catchment and does not receive waters from any freshwater stream; and (2) nearly all of its tidal flows are constrained through a single channel by a road that acts as a levee. During five intensive sampling periods, hourly samples were collected from that single outlet for approximately 40 continuous hours (three semi-diurnal tidal periods) throughout 2007 and 2008. We then determined net fluxes between this marsh and Murderkill Estuary for each of the measured parameters, using a newly developed approach that substantially reduces the propagation of errors that are amplified when taking the difference between the large inflows and outflow. We believe this new approach to calculating loads has global applicability to all tidal systems and has particular applicability to well-mixed and/or turbid estuarine systems.

The **motivation** for this study is to extrapolate our marsh flux results to all other salt marshes in the Murderkill Estuary, then to use those net marsh loads to calibrate and to test the assumptions of a hydrodynamic/water-quality model for the Murderkill River and Estuary. This extrapolation and modeling work has been done by other members of the Murderkill Study Group (<http://whiteclay.wra.udel.edu/murderkill/>).

The results of the related work for our project on water and salt balances on Webbs Marsh in the Murderkill Estuary has been previously reported to the Kent County Board of Public Works (Report Parts A & B: Wong et al., 2009; Dzwonkowski et al., 2011, 2013).

2.2 Background: Murderkill Watershed and Estuary

The Murderkill Watershed and Estuary are located in southeastern Kent County, Delaware. The Murderkill Estuary drains a 275 km², primarily agricultural (55% as of 2002; DNREC, 2004, 2006), watershed and discharges to Delaware Bay (Figure 1). The soils are permeable and well-drained and groundwater recharge potential is good to excellent over much of the watershed, consistent with the coastal plain setting (DNREC, 2006; Andres, 2004). Approximately 11% of the watershed is covered by forest and 14% is urban/built-up (DNREC, 2006). 17% of the watershed is covered by wetlands, of which 36% are tidal, and 60% are freshwater (including forested wetlands; DNREC, 2004, 2006). The Kent County Wastewater Treatment Facility (KCWTF) that treats wastewater originating from throughout the Kent County,

including the principal urban centers of Dover, Smyrna, and Milford, discharges directly to the Murderkill Estuary. As a consequence of the discharge through KCWTF, the Murderkill Estuary effectively has a higher population burden than implied by the land use of its own watershed. During the period of this study, the Harrington wastewater treatment facility also discharged to the headwaters of Browns Branch, although this wastewater has now been redirected to the KCWTF. Most of the rural development disposes of its waste through domestic septic and small community systems (DNREC, 2001a).

The drainage system of the watershed consists of three tributaries (Figure 1). Spring Creek, to the north contributes approximately 23% of the total discharge that reaches the Estuary. The Murderkill River and Browns Branch, to the south, contribute the remaining 64% (De Michele, 1972; cited in deWitt and Daiber, 1974). The remaining 13% enters from streams and subsurface pathways draining to and through the extensive marshes bordering the Murderkill Estuary (De Michele, 1972; cited in deWitt and Daiber, 1974). The tributary streams have extensive riparian boundaries, including riparian forests and marshes.

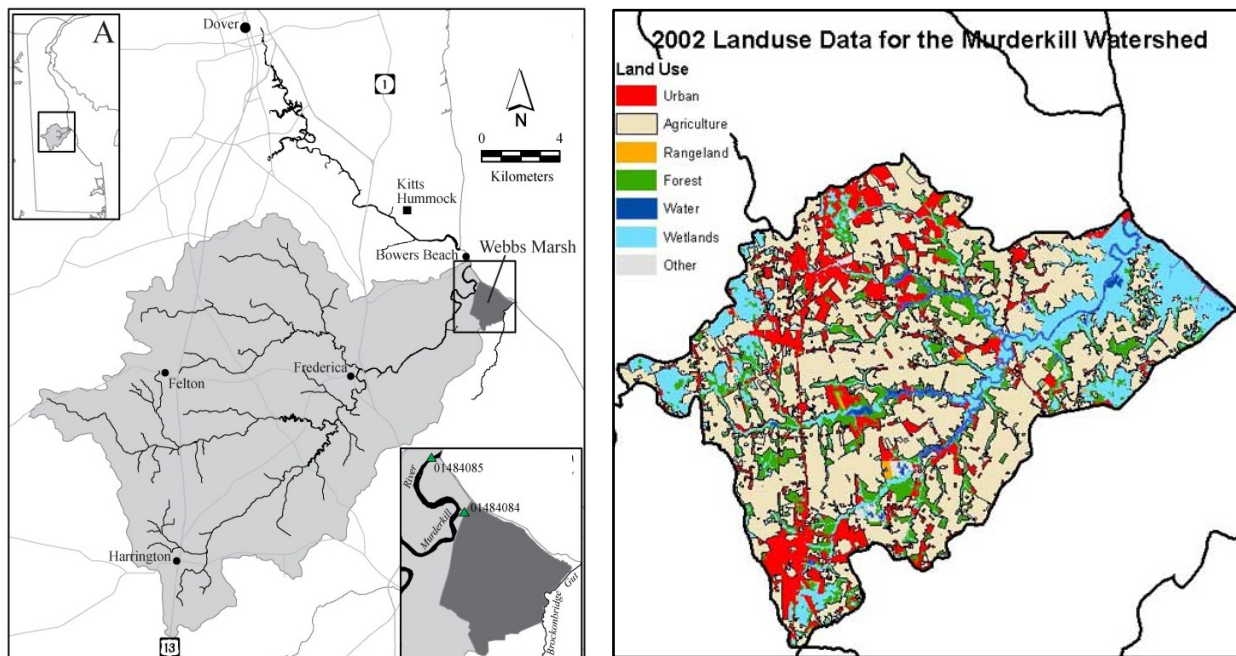


Figure 1. Location of the major features of the Murderkill Watershed. (A) Watershed boundaries showing the main tributaries to the Estuary, with inset showing approximate boundaries of Webb's Marsh, and the location of USGS Gauging Station 01484084 (Unnamed Ditch near Webb Landing). (B) Principal land uses of the Murderkill Watershed (2002 DNREC data).

In recent years, many stream segments and ponds have been classified as impaired by the Clean Water Act (NRCS, 2007) and, since 2001, the State of Delaware has proposed and promulgated Total Maximum Daily Load (TMDL) regulations for nutrients, oxygen-consuming compounds, and bacteria designed to improve watershed and estuarine water quality with the goal of meeting federal Clean Water Act and State of Delaware water quality standards (DNREC, 2004, 2006).

Based on data collected between 1967 to 1970, prior to the construction of the present KCWTF, the mean flushing time of the Murderkill Estuary is about 55 hours, but varied from 32 hours (at high flow) to 230 hours (at low flow; deWitt and Daiber, 1974). The horizontal salinity distribution of the Estuary is dependent on the balance between tidal inputs from Delaware Bay and discharge from the Murderkill Watershed (deWitt and Daiber, 1974). At high tides and/or low runoff, up to 50% of the lower part of the Estuary is occupied by a fairly homogeneous watermass originating from Delaware Bay (and thus variable in salinity on longer time scales due to freshwater discharge to and estuarine mixing in this larger system). At low tides and/or low runoff, fresh water from the Murderkill Watershed may occupy up to 50% of the upper Estuary. In between the Delaware Bay and Murderkill Watershed endmembers is a mixing region with a steep salinity gradient that varies in position and intensity with the hydrology. The Estuary has minor vertical salinity gradients and therefore has characteristics intermediate between the classic definitions of well-mixed and partially stratified estuaries (deWitt and Daiber, 1974). DeWitt and Daiber (1974) reported high turbidity levels (based on Secchi disk measurements ranging from 15-60 cm) with both watershed and Delaware Bay sources of suspended sediments; turbidity was higher in the summer than in winter. Dissolved oxygen concentrations also varied seasonally with temperature and reached their minimum during the summer months with concentrations below 4 mg/L measured in the middle sections of the Estuary. Similar conditions were observed during the 2007 and 2008 sampling period.

Most of the Estuary has been classified as impaired by the Clean Water Act (NRCS, 2007; DNREC, 2004, 2006).

3 Approach and Methods

3.1 Sampling Site

All samples were collected at the USGS gauging station on the channel connecting Webbs Marsh to the Murderkill Estuary ([USGS Station 01484084](#), Unnamed Ditch near Webb Landing at South Bowers, DE, [39.050333°N, -75.391306°W](#)). The gauging station was located at a bridge on South Bowers Road, approximately 1 km south-southeast of Bowers, DE, and approximately 90 m from the confluence of the channel and the Murderkill Estuary (Figure 2). Webbs Marsh is 0.64 km² in area (McKenna, T.E., personal communications), has no significant upland catchment and does not receive waters from any freshwater stream.

The channel under the sample bridge is the principal connection between Webbs Marsh, the Murderkill River/Estuary and Delaware Bay as South Bowers Road serves as a levee between the marsh and the Murderkill River. However, there are some distal channels to the south of Webbs Marsh that may discharge to the next tributary to the south, Brockenbridge Gut following very high tides (T.E. McKenna, personal communication). There is also a culvert under South Bowers Road, approximately 400 m south-southwest of the sampling site that may transport water in and/or out of the Webbs Marsh following high tides, although the flows are likely small due to the small size of the culvert. Evidence discussed below suggests that during very high tides there is some water that enters the marsh through the channel connected to the Murderkill Estuary that exits the marsh through some other pathway after very high tides. There is also



Figure 2. Webbs Marsh is a 0.64 km² salt marsh that drains primarily into the tidal Murderkill River under the bridge at South Bowers Road, which acts as a levee on the western side. Webb's Slough is a drainage ditch network dug in the 1930's, which does connect to Brockenbridge Gut during some high tides. Map courtesy of T.E. McKenna.

evidence that at very high tides, some water enters the marsh by pathways other than this channel, due to flooding of the marsh surface leading to cross basin exchange.

3.2 Sampling Dates and Times

Water samples were collected hourly for 39 to 40 hours on five occasions during 2007 and 2008 at the Webbs Marsh sampling site (Table 1). Sampling dates were chosen based on when predicted tides would have moderate amplitudes, avoiding spring and neap tides. During the last sampling period, samples were also collected at some other stations beyond the marsh (MKF).

Table 1. Sampling at the Webbs Marsh site, Murderkill Estuary, Delaware

Sampling	Dates and Times (Local Time)	Number of Hourly Samples	Comments
MKA	16 Jul 07 14:35 to 18 Jul 07 4:00	38	Early Summer
MKB	17 Oct 07 6:02 to 18 Oct 07 18:06	40	Fall
MKC	1 Apr 08 6:12 to 2 Apr 08 21:02	40	Early Spring; Blow-out tides
MKD	14 May 08 6:00 to 15 May 08 20:02	39	Late Spring; Blow-in tides
MKE	13 Aug 08 6:02 to 14 Aug 08 20:05	39	Late Summer
MKF	12 Aug 08 15:07 to 14 Aug 08 1:22	9 Spatial Samples (KCWTF, Bowers, Webb Landing)	

3.3 Approach

Our objectives required the quantitative analysis of concentrations of all major dissolved and particulate species transported to and through the Webbs Marsh gauging site for the bioactive elements oxygen, carbon, nitrogen and phosphorus. We analyzed stable isotopes of a number of these species to provide additional information about sources. We analyzed a number of other physical, geochemical and biological parameters to provide context and additional information on water sources, conservative mixing and mass balance. Measured species, their purpose and our analytical method used to measure them are all listed in Table 2.

3.4 Sampling Methods

During each intensive sampling period, water samples were collected every hour on the hour for 38 to 40 continuous hours by suspending a submersible pump from the bridge into the center of the channel to approximately 6/10 of the total depth. The water was pumped at 4-8 L/min. While the pumped water was used to rinse out the various sampling containers, a small fraction of the flow (~ 0.1 to 0.2 L/min) was used to fill a 0.25 L plastic bottle that served as a flow-through chamber for pH. The flow-through container was filled from the bottom to minimize gas exchange. Dissolved oxygen, conductivity/salinity and temperature were determined in the channel using a YSI Model 85 meter. After all values stabilized and were recorded, three groups of sample bottles were filled directly from the pump outflow: a 1 L bottle for subsequent processing for dissolved nutrients, a 10 L carboy for the determination of suspended sediment and particulate carbon, nitrogen and phosphorus concentrations, and a pair of 12 mL glass Exetainer™ vials for dissolved inorganic carbon. These bottles were immediately processed in our field lab – a recreational vehicle and screen tent set up within 20 meters of the collection site. Last, a 63 µm plankton net was deployed from the bridge for ~5 minutes in order to collect coarse suspended sediment (CSS > 63 µm) for compositional analysis.

Dissolved sample processing. The water samples for dissolved nutrients (nitrate, ammonium, phosphate, silica, total dissolved nitrogen, and total dissolved phosphorus) were manually filtered via vacuum filtration through a 47mm Whatman GF/F filter into a clean 125-mL polyethylene bottle that was rinsed once with sample water. The silica samples were decanted out of this bottle into clean 20-mL polyethylene scintillation vials, which were also rinsed once

Table 2. Nutrient, carbon, and related parameters to be determined for the purpose of measuring net seasonal fluxes to and from the Murderkill River Estuary and identifying the major biogeochemical and hydrological factors controlling these fluxes.

Element	Species	Purpose	Analytical Technique(s)*
Carbon	DOC	Mass Balance	TOC-IRMS †
	$\delta^{13}\text{C}$ of DOC	Provenance/Biogeochemistry	TOC-IRMS †
	Fine & Coarse POC	Mass Balance	CHN-IRMS †
	$\delta^{13}\text{C}$ of POC	Provenance/Diagenesis	CHN-IRMS †
Nitrogen	NH_4^+	Biogeochemistry	Wet chemistry ‡
	$\text{NO}_2^- + \text{NO}_3^-$	Biogeochemistry	Wet chemistry ‡
	TDN	Mass Balance	As NO_3^- after persulfate oxidation ‡
	$\delta^{15}\text{N}$ & $\delta^{18}\text{O}$ of NO_3^-	Provenance/Biogeochemistry	GasBench IRMS †
	Fine & Coarse PON	Mass Balance	CHN-IRMS †
	$\delta^{15}\text{N}$ -PON	Provenance/Biogeochemistry	CHN-IRMS †
Phosphorus	PO_4^{3-} (orthophosphate)	Biogeochemistry	Wet chemistry ‡
	TDP	Mass Balance	As PO_4^{3-} after persulfate oxidation ‡
	PP	Mass Balance	Wet chemistry after combustion ‡
Physical Parameters	Salinity	Mixing	Handheld YSI 85 Meter
	Temperature		
	Dissolved O_2	Oxygen Excess/Deficit	
Other	Chlorophyll <i>a</i>	Provenance/Biogeochemistry	Acetone Extraction and Fluorescence ‡
	Dissolved Si	Mass Balance	Wet chemistry ‡
	Alkalinity	Porewater tracer and DIC speciation	Auto-titration †
	Fine and Coarse Suspended Solids	Mass Balance	Gravimetry †

* Abbreviations: DOC = Dissolved Organic Carbon; POC = Particulate Organic Carbon; TDN = Total Dissolved Nitrogen; TDP = Total Dissolved Phosphorus; PP = Particulate Phosphorus; CHN= Carbon, Hydrogen, Nitrogen Analyzer; IRMS = Isotope Ratio Mass Spectrometer

† Analyses performed at Stroud Water Research Center.

‡ Analyses performed at the University of Delaware.

with sample water. Water samples for dissolved nutrients in the 125-mL bottles were frozen within 30 minutes of collection and kept in the freezer until they could be analyzed. The silica samples in the 20mL vials were kept in the refrigerator until they were analyzed.

Particulate sample processing. Immediately after collection, the volume of the graduated 10-L carboy was measured and its contents were poured into a churn sample splitter (Bel-Art, Wayne, NJ) through a 63 μm sieve to separate coarse suspended sediment (CSS > 63 μm) from fine suspended sediment (FSS, 0.45-63 μm). The churn sample splitter was then used for all subsampling of the fine suspended sediment fraction to ensure equal concentrations of particles in all subsamples (Lane et al., 2003). Duplicate samples for FSS were filtered onto a pair of stacked pre-weighted membrane filters (Millipore HAWP; nominal pore-size of 0.45 μm). Samples for determination of POC/PON were collected on 47 mm glass fiber filters (Millipore AP40; nominal pore-size of 0.7 μm). CSS collected on the sieve were washed onto a similar set of pre-weighed filters. All particulate samples were refrigerated within an hour of sample collection and then dried in a 60°C oven upon returning to the lab. Samples for Chlorophyll a (Chla) and PP were collected on 25 mm glass fiber filters (Whatman GF/F) and frozen prior to analysis.

3.5 Analytical Methods

Dissolved Sample Analysis. An O/I Analytical Flo-Through Analyzer (College Station, TX) was used to analyze water samples for Nitrate + Nitrite (hereafter: Nitrate), Ammonium, Total Dissolved Nitrogen, and dissolved Silica (hereafter Silica). Phosphate and total dissolved phosphorus were analyzed manually on a Milton Roy 701 spectrophotometer. Standard oceanographic methods were used for sample analyses, as described in detail in Hays (2009).

DOC and DIC concentrations and stable carbon isotope composition were measured on an O/I Analytical Total Organic Carbon (TOC) Analyzer model 1010 coupled to a Thermo DeltaPlus XP Isotope Ratio Mass Spectrometer (IRMS) via an interface box consisting of a heated copper reduction column (600C) to reduce N_2O to N_2 and a gas chromatography column using the methods of St-Jean (2003) and Osburn and St-Jean (2007). Standard curves for the elemental and isotopic analysis were created for each batch using 8 or 9 isotopically enriched (+37.63‰) and depleted (-26.39‰) L-glutamic acid standards over a range of carbon masses that encompassed the subsample masses, enabling accurate blank correction. Stable carbon isotope ratios, reported using $\delta^{13}\text{C}$ notation, were normalized relative to the Vienna Peedee Belemnite standard using a 2-point approach (Coplen et al., 2006).

Particulate Sample Analysis. After drying filters 12-18 h at 60°C to constant mass, CSS and FSS concentrations were quantified as the change in the mass of the top filter (i.e. sediment mass, solute mass and balance drift) minus the change in mass of the bottom filter (i.e. solute mass and balance drift) all divided by the filtered water volume. The average error of field duplicates of FSS was $\pm 3.8\%$.

CSS and FSS samples collected on glass fiber filters were uniformly subsampled with a cork bore, wetted with nanopure water and fumed with hydrochloric acid vapors for 18 hours, effectively removing carbonates while eliminating nitrogen contamination via vapor phase ammonia (A. K. Aufdenkampe unpublished). Subsamples were analyzed in batches on an

Elemental Analyzer (Costech ECS 4010) interfaced with an Isotope Ratio Mass Spectrometer (Thermo DeltaPlus XP). Standard curves were developed for each batch using reference materials and methods as described above for DOC-IRMS. POC concentration (mg C L^{-1}) was calculated from the mass of C analyzed, the fraction of total sample analyzed, and the volume of stream water filtered. Weight percent organic carbon of fine suspended sediment (carbon content) was calculated as the ratio of POC (mg POC L^{-1}) to FSS (mg FSS L^{-1}) concentrations. These methods were adapted from Aufdenkampe et al. (2001, 2007) and Richardson et al. (2009).

4 Results and Discussion

4.1 Sampling Period Conditions: Normal vs. Episodic Events

The goal of this work was to estimate nutrient, carbon, and oxygen hourly loads to and from Webbs Marsh under conditions normally found in the Murderkill Estuary, from which to estimate loads for longer time intervals. Sampling was designed to occur at mid-level tides away from spring and neap tides and sampling dates were chosen based on predicted tides. However, once a sampling date was chosen, it was not easily changed due to the preparations required and the number of people involved in the sampling. Thus, it is not surprising that some of the sampling occurred during episodic events that differed significantly from the expected tides (Table 1). Samples collected on 1-2 April 2008 (MKC) reflect a period of upwelling favorable winds at the mouth of Delaware Bay that drew water out of Delaware Bay, leading to significantly lower tidal heights than predicted and substantially lower salinities than expected (Wong et al., 2009). Samples collected from 14-15 May 2008 (MKD) reflect a period of downwelling favorable winds at the mouth of Delaware Bay that forced coastal water up into the bay. This sampling period also followed immediately after the Mother's Day Storm of 2008 that brought a large amount of rainfall and local flooding as well as near-record high tides to the Murderkill Watershed (11-13 May 2008; <http://www.erh.noaa.gov/phi/storms/05132008.html>). The data and results reported here reflect the conditions at the time of sampling and due to the lack of more extensive data sets, we must use our measured values with this knowledge in mind as we estimate loads for the project period outside of our sampling dates. For example, for our estimates of mean annual fluxes of most species we excluded data from MKD in the average. However, when we estimate fluxes based directly or indirectly on the continuous data collected by USGS that captured many storm events, the data that we collected during MKD were invaluable in our understanding of the processes that can occur during storms.

4.2 Concentrations as a Function of Tidal Stage: Period MKA as an Example

The analytical results of the MKA sampling (16-18 July) are shown for illustration of our approach to interpreting concentration data relative to physical flow data for eventual calculation of loads. Figure 3 shows the physical measurements made at the Webbs Marsh site. Gauge height, discharge and salinity were determined by USGS. Discharges here reflect the instantaneous discharge determined on each hour during the MKA sample period. There is good agreement between the continuous temperatures measured by USGS (black line) and the hourly measurements made by our group. There is a larger discrepancy between salinity and

dissolved O₂ determinations made by the USGS and our group. As a result, salinity and O₂ data from the two sources were not comingled. We use our own salinity data in all of our analyses. This choice does not affect the quality of the load estimates.

There is a marked asymmetry in the discharge from Webbs Marsh. Ebb tides are longer than flood tides (Dzwonkowski et al., 2011, 2013). Salinity also follows a repeatable, but not strictly tidal pattern, with time. This pattern results from the changing input to Webbs Marsh as a function of tide propagation into the Murderkill Estuary and its marsh channels and the infiltration and storage of water in tidal creek banks (Howes and Goehring, 1994; Gardner, 2005; Wilson and Gardner, 2006). The first water to enter the marsh from the Estuary at the beginning of flood tide reflects the low salinity water that propagated downstream in the Estuary at the end of the previous ebb tide. As the tide level rises, the water entering the marsh becomes more saline and more constant as Delaware Bay water reenters the Estuary and marsh channel. The water entering the marsh channels reverses the hydraulic gradient between the channel and the channel banks and the flooding water infiltrates through burrows and root channels into the channel banks (Howes and Goehring, 1994; Gardner, 2005; Wilson and Gardner, 2006). At the beginning of ebb tide, the water exiting the marsh is similar to the water that entered the marsh at the end of the previous flood tide. This leads to a long period of essentially

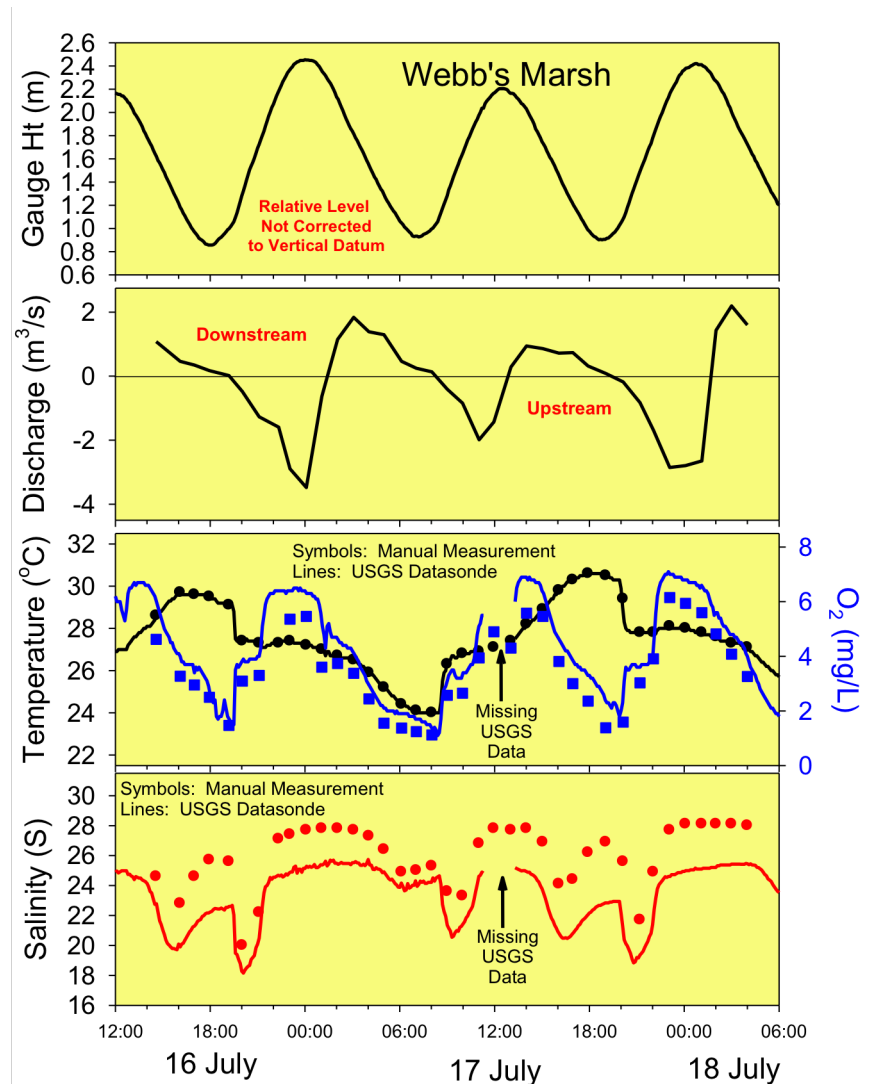


Figure 3. Physical measurement made at the Webbs Marsh site during the MKA sampling period (16 to 18 July 2007). Gauge height, instantaneous discharge on each hour, temperature, and salinity were made by USGS. There is good agreement between simultaneous measurement of temperature made by USGS and our group. There is a noticeable discrepancy between salinity and dissolved O₂ estimates made by the two groups (see text).

constant and high salinity during each tidal period reflecting the common origin of these waters (Figure 3). As the tide continues to ebb, however, some the lower salinity water that filtered into the creek banks during the early stages of the preceding flood tide is added to the channel. Last, there is usually another peak in salinity corresponding to the return of some higher salinity water that propagated into the distal areas of the channel and marsh during the previous flood leading to a second minor salinity peak. This distinctive pattern of two peaks and two valleys in salinity over each tidal cycle that is observed to a greater or lesser extent during all sampling periods and during the entire USGS salinity record at this site (Eickmeier et al., in preparation).

Although this pattern is seen distinctively in the tidal channel due to the relatively large volume of water that infiltrates into tidal creek banks during flood tide and is then released

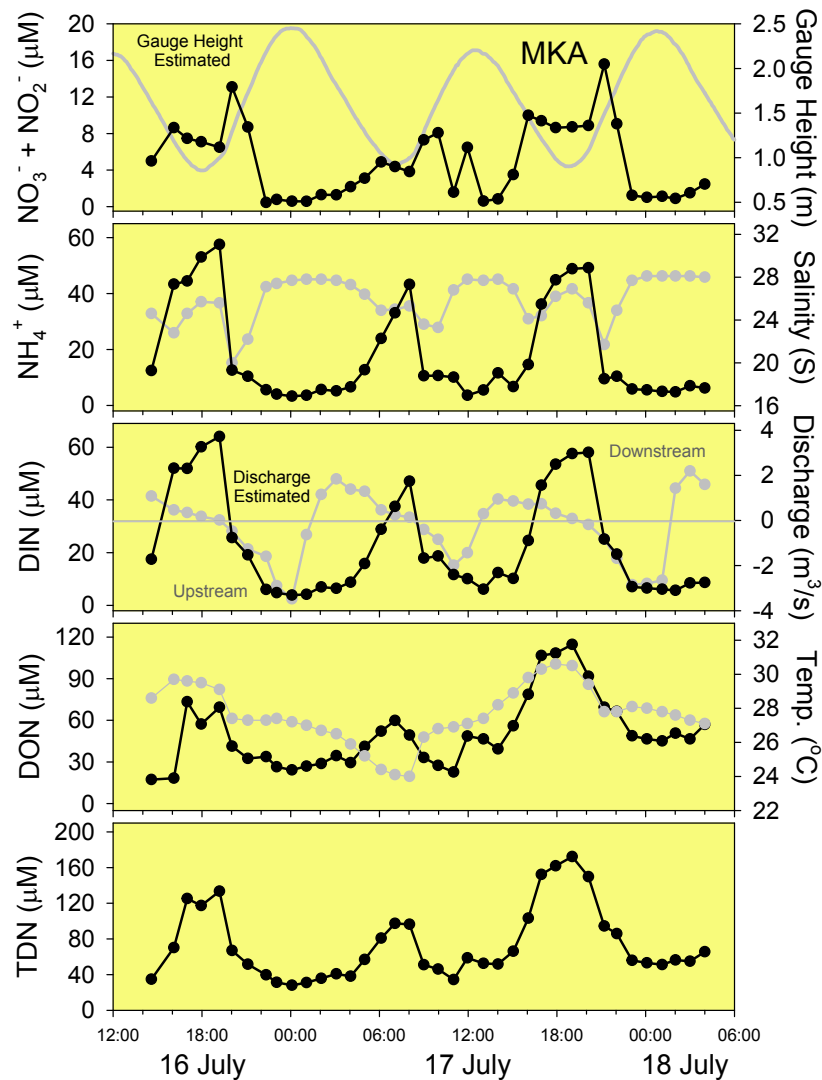


Figure 4: Concentrations of nitrogen species collected from 16 to 18 July 2007 at the Webb's Marsh gauging station. The patterns of NO_3^- reflect the changing estuarine source as a function of tidal mixing and that the first water in (low salinity) to the marsh is also the last water out. Gauge height, salinity, discharge, and temperature data are shown in light gray.

during ebb tide, it is not seen in the Murderkill Estuary with the infiltration volume is dwarfed by the large tidal flow (Eickmeier et al., in preparation). The infiltration of flood tidal water into the channel banks and discharge of this water during ebb tide also helps to explain the patterns of nutrient release from Webb's Marsh.

Figure 4 shows the concentrations of nitrogen species during the MKA sampling period. Nitrate follows a repeatable, but not simply tidal pattern with time. The lowest concentrations are typically found at high tide reflecting the lower nutrient concentrations found in Delaware Bay water as compared to the Murderkill Estuary. The highest NO_3^- concentrations co-occur with the lowest salinities, reflecting contributions of waters with relatively high nitrate concentrations from the Murderkill Watershed and from the KCWTF that both enter the marsh from the Estuary at the

beginning of flood tide. There is also a minor secondary peak toward the end of ebb tide that reflects the return of water from channel margins that was recharged with NO_3^- -rich waters during the previous flood tide. Ammonium (NH_4^+) and dissolved organic nitrogen (DON) are low in the Delaware Bay and estuarine waters but high in the effluent waters from the marsh, particularly toward the end of ebb tide, consistent with the discharge from the tidal banks of interstitial water produced during suboxic and anoxic degradation of sedimentary organic matter. These reduced species actually dominate the inorganic and total dissolved nitrogen

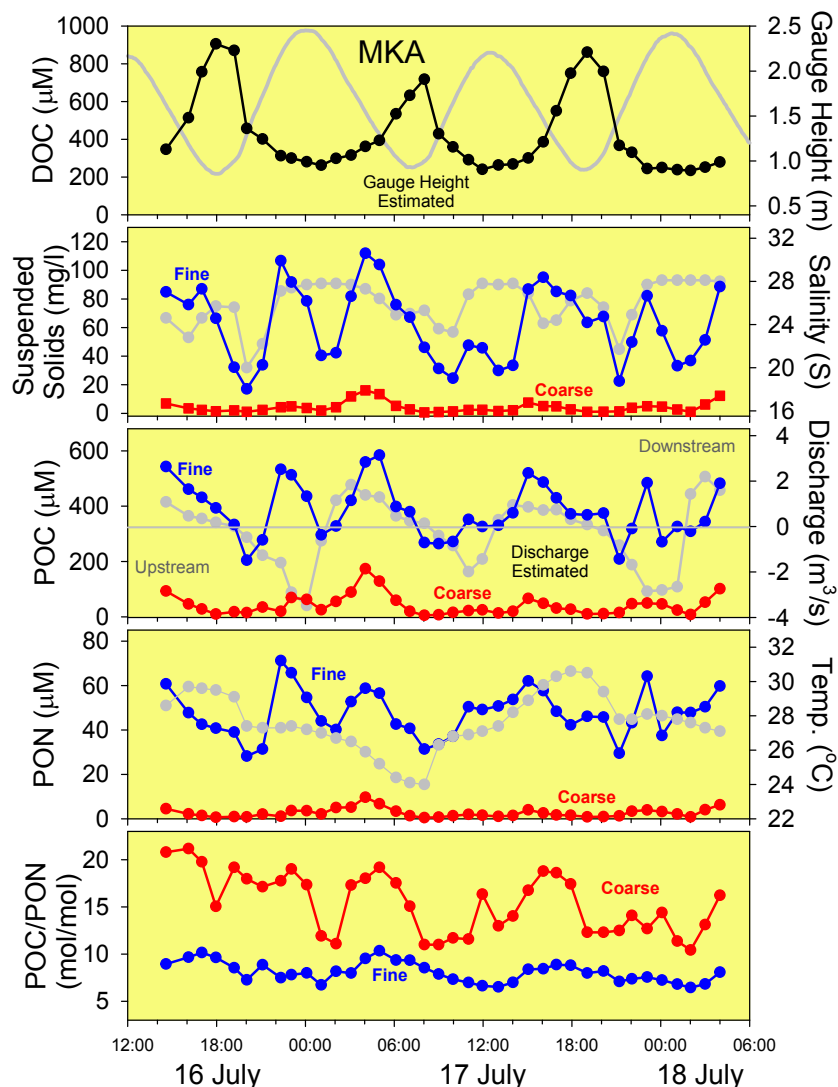


Figure 5. Observed distribution of dissolved organic carbon (DOC) and suspended solids, particulate organic carbon (POC) and nitrogen (PON) in both the fine and coarse size fractions from 16 to 18 July 2007. The distribution of DOC is clearly related to distributions of NH_4^+ , DON, and Si (see below) that similarly result from anoxic and suboxic diagenesis. Fine particulate matter and associated PON and POC appear to be remobilized from the channel boundaries by high tidal velocities. Gauge height, salinity, discharge, and temperature data are shown in light gray.

speciation at ebb tide. The large increase in NH_4^+ , DIN, and DON, and TDN – species that are typically elevated in sedimentary pore waters due to suboxic and anoxic diagenesis – is evidence of mixing between surface waters and sedimentary porewaters along channel banks and the importance of this process as a mechanism of nutrient exchange with surface waters (Howes and Geohringer, 1994; Gardner, 2005; Wilson and Gardner, 2006). As the increase in concentration of these reduced species is substantially larger than the highest observed NO_3^- concentration, the reduction of NO_3^- originating with surface waters cannot alone be a substantial contribution to the N load from the marsh back to the Estuary.

Figure 5 illustrates the patterns of particles, particulate nitrogen and carbon, and dissolved organic carbon exchange between Webbs Marsh and the Murderkill Estuary. One peak in DOC concentration is seen at the end of each tidal cycle

as seen for NH_4^+ , DON (Figure 4), and Si (see Figure 8 below). In contrast, coarse ($>63 \mu\text{m}$) and fine ($0.7\text{-}63 \mu\text{m}$) suspended solids, POC and PON concentrations increase around the peaks of tidal recharge and discharge, responding to the high average velocities in the tidal channel during the most rapid change in tidal height during ebb and flood tides: two peaks are seen in the concentrations of suspended solids, fine-grained PON and POC (FPON and FPOC) and, to a lesser extent, in coarse-grained PON and POC (CPON and FPOC) during each tidal cycle. This would suggest that a primary control on particle concentration at the Webbs Marsh site is turbulent shear-driven erosion and suspension of the bed and banks of both the Murderkill River and channels within the marsh during peak tidal flows. The POC/PON ratios indicate differences in the sources and diagenesis of fine and coarse particles. The fine particles have molar C/N ratios ranging from 6.5 to 10.3, which is consistent with the

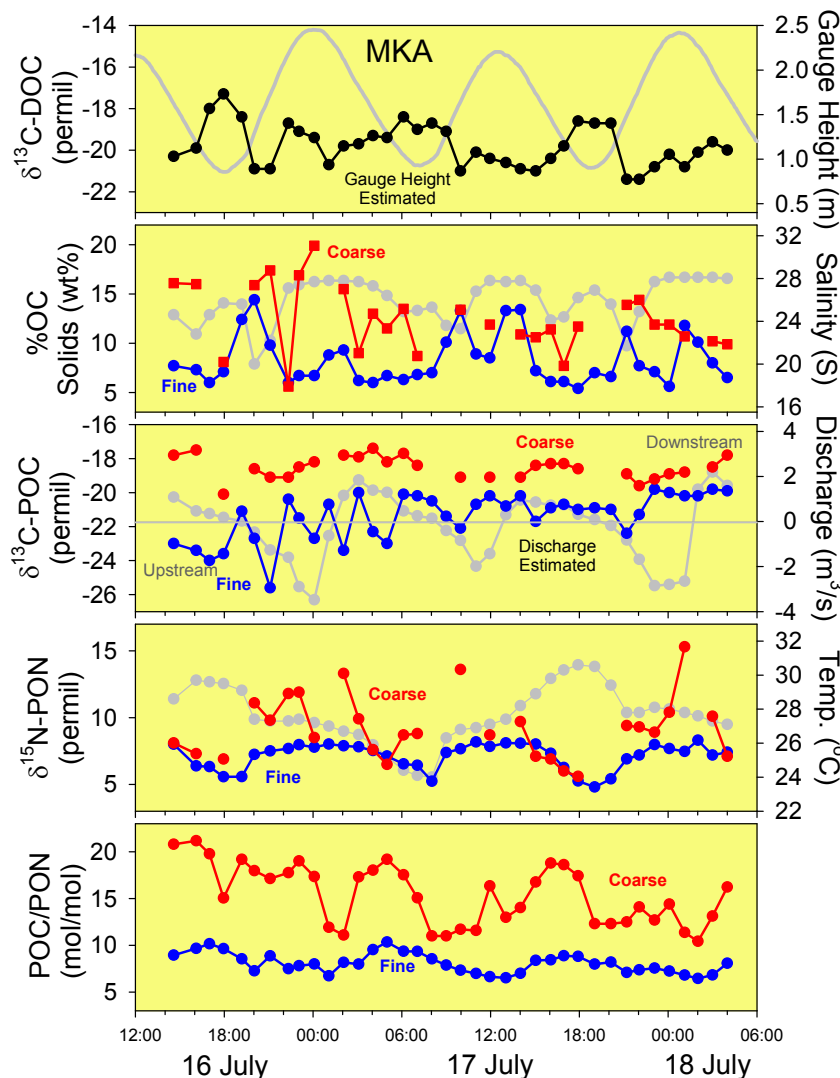


Figure 6. Organic matter compositional characteristics, including stable isotopes and elemental composition from 16 to 18 July 2007. Course particulate samples were often not collected in sufficient quantity to complete all analyses, as indicated by missing values. Gauge height, salinity, discharge, and temperature data are shown in light gray.

composition that is a combination of marine phytoplankton ($\text{C/N} \approx 6.6$) and soil organic matter ($\text{C/N} = 7\text{-}12$). The coarse particles have C/N ratios ranging from 11.1 to 21.1, consistent with likely contributions from vascular plant detritus ($\text{C/N} = 15\text{-}60$) as is observed in most riverine systems (Aufdenkampe et al., 2007).

Figure 6 shows elemental and isotopic compositions of organic matter in transport. The $\delta^{13}\text{C}$ of DOC shows maximum values of -17‰ to -19‰ at the end of ebb tide, the same period when DOC, NH_4^+ and Si concentrations are at a maximum. During early flood tide $\delta^{13}\text{C}$ of DOC decreased to -21‰ . CPOM had similar $\delta^{13}\text{C}$ signatures and temporal patterns compared to DOM over the tidal cycle, but over a smaller range. FPOM had much more depleted $\delta^{13}\text{C}$ than DOM, ranging from -26‰ to -20‰ . The $\delta^{13}\text{C}$ signatures of possible end-members

include: (1) warm-climate terrestrial grasses, including *Spartina spp.*, that use the C-4 photosynthetic pathway and have $\delta^{13}\text{C}$ of -12‰ to -14‰ ; (2) marine and estuarine algae that have $\delta^{13}\text{C}$ of about -20‰ ; and (3) most other terrestrial plants, including all broad leaves and cool-season grasses, that use the C-3 photosynthetic pathway and have $\delta^{13}\text{C}$ of -27‰ to -28‰ . Therefore, DOC and CPOC both have clear contribution from C-4 grasses and FPOC has a clear contribution from C-3 plants. However, one isotope cannot be used with three end-member sources for either exact quantification of carbon contribution from each or exclusion of one. Weight percent carbon and C/N ratio both suggest that CPOM is primarily composed of moderately degraded leaf detritus, whereas FPOM is likely highly processed organic matter that is more tightly associated with minerals (Aufdenkampe et al., 2007). Thus, fine vs. coarse suspended sediment fractions appear to have contrasting sources and history, whereas DOM and CPOM both appear to have similarly substantial contributions from salt marsh grasses such as *Spartina spp.*

Figure 7 shows dissolved oxygen concentrations, the calculated partial pressure of carbon dioxide (pCO_2), and the measured titration alkalinity and measured pH used to calculate the pCO_2 using the salinity and temperature dependent equilibrium constants for the dissociation of carbonic acid (Millero, 1979, 1995; Fofonoff and Millard, 1983; Zeebe and Wolf-Gladrow, 2001). Dissolved O_2 (DO) ranged from 1.1 to 6.2 mg/L and showed a tidal pattern similar to NH_4^+ , DOC and Si but opposite in direction, in which DO reached a minimum as the last tidal waters drained the marsh. The partial pressure of

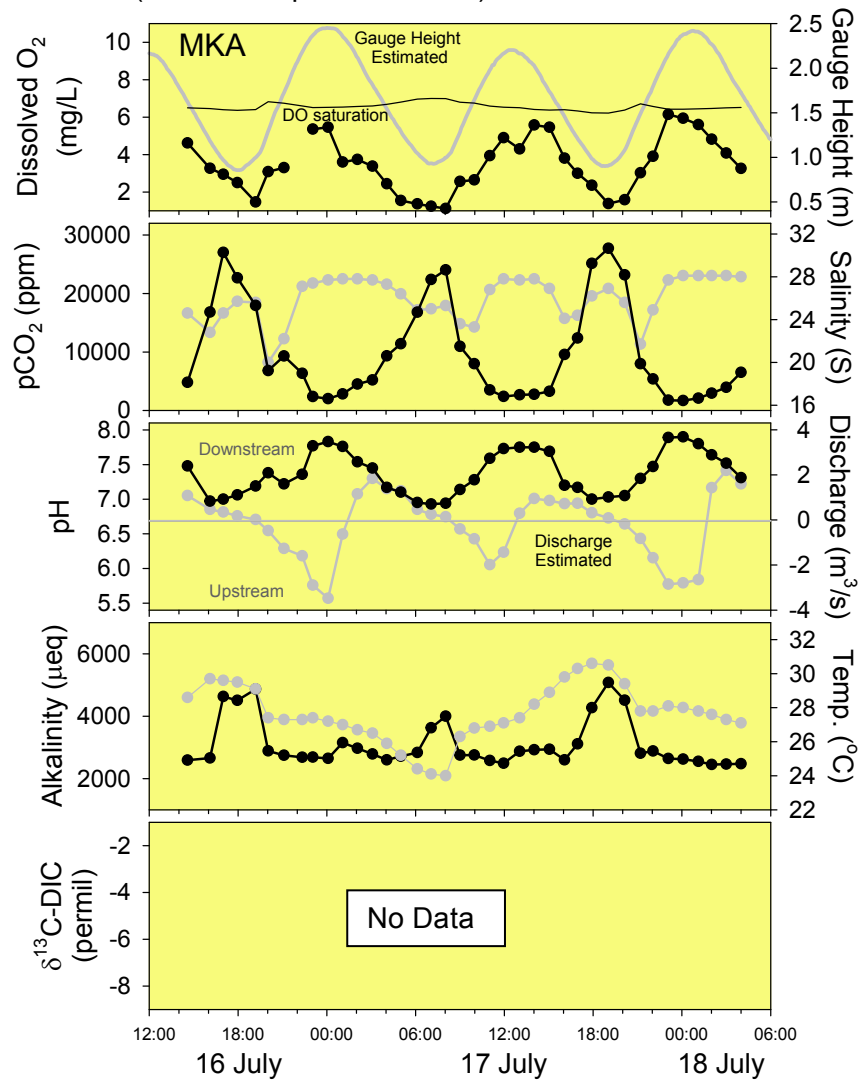


Figure 7. Dissolved O_2 , the partial pressure of dissolved free CO_2 (pCO_2), and pH and total alkalinity, which were used to calculate pCO_2 , from 16 to 18 July 2007. $\delta^{13}\text{C}$ of DIC was not measured for MKA and the lower panel is intentionally black for comparison to plots where it was measured, for MKB and MKC, shown below. Gauge height, salinity, discharge, and temperature data are shown in light gray.

dissolved free CO₂ (pCO₂) ranged from 2250 to 33,700 ppm, or 6-86x super-saturation relative to an atmospheric concentration of about 390 ppm. These extreme disequilibria between the atmosphere and dissolved O₂ and CO₂ strongly suggest that equilibration time between these waters and the atmosphere has been very limited. Given that DO and pCO₂ are most out of equilibrium at the very end of ebb tide when water levels are lowest – the same moment when total alkalinity, NH₄⁺, DOC and Si are all at a maximum in concentration – strongly suggests that marsh sediment pore waters as the source. δ¹³C of DIC was not determined for MKA samples but was for MKB and MKC samples (data shown below).

Figure 8 shows the patterns of soluble reactive phosphorus (SRP; ≈ ΣPO₄³⁻) and silicate (Si) concentrations as a function of time, tide height, and salinity at the Webbs Marsh gauging station. In contrast to all of the rest of the dissolved nutrients, SRP concentrations show two tidal peaks that correspond to suspended sediment peaks during high velocity tidal flows (Figure 5) and also to periods of relatively lower salinity. SRP found in the oligohaline and mesohaline waters of the Murderkill Estuary is relatively high due to contributions from both the watershed and from the KCWTF. In contrast, SRP dips again during the low ebb tide discharge when NH₄⁺, DON, and Si increase (Figures 4 and 8) due to release from the marsh sediment. The similarity in the observed PO₄³⁻ concentrations in the inflow and effluent waters suggest that exchange of interstitial waters between the marsh channel and channel margin is a relatively small source of PO₄³⁻ compared to nitrogen (NH₄⁺ and DON; see Figure 4). In contrast, Si release appears to coincide with the release of other nutrients from the marsh and marsh channel banks. Concentrations in the surface waters of the Murderkill Estuary are apparently consistently low in Si, compared to the marsh sources.

From these data, a consistent picture of the processes controlling the concentrations of biogeochemically active dissolved species and, in some cases, the isotopic composition of these species emerges:

waters that interacted with marsh sediments the longest – by flowing through sedimentary pores – showed signs of mineral dissolution through higher Si and alkalinity concentrations, substantial heterotrophic mineralization of sedimentary organic matter through very low oxygen and very high pCO₂ and NH₄⁺ concentrations, and substantial organic matter leaching and export as DOC. These products of anoxic and suboxic diagenesis drained from the marsh at the very end of ebb tide when water levels

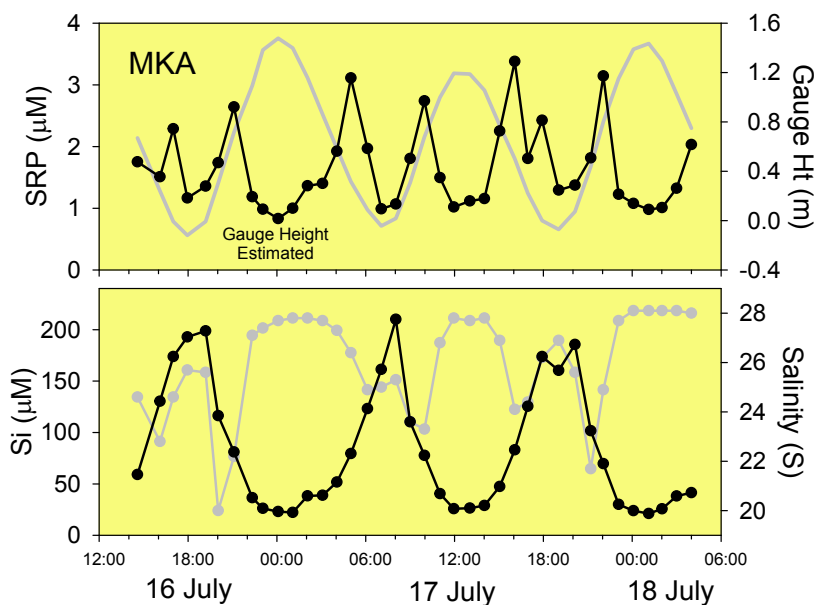


Figure 8. Concentrations of soluble reactive phosphorus and Si collected from 16 to 18 July 2007 at the Webbs Marsh gauging station. Gauge height and salinity are shown in light gray.

were the lowest, reflecting the importance of physical processes in the exchange of bioactive nutrient species between the Webbs Marsh platform, the marsh banks, marsh channel and the Murderkill Estuary.

4.3 Concentrations as a Function of Tidal Stage: Other Sampling Periods

Figure 9 shows the distribution of dissolved nitrogen species for the MKB, MKC, MKD and MKE sampling dates (October 2007, April 2008, May 2008, and August 2008, respectively). In October 2007 (MKB) the ranges of concentration in nitrogen species are similar to those observed in July 2007 (MKA). In both cases NH_4^+ and DON dominate the nitrogen speciation. The double peaks in NO_3^- concentration are seen during both sampling periods, although the two peaks are more comparable in magnitude during October than in July. This would suggest that the consumption of NO_3^- during bank infiltration-exfiltration is lower in the cooler weather.

In April 2008 (MKC), concentrations of all dissolved nitrogen species are higher than measured on any other sampling dates. This is probably related to three factors: (1) the lack of photosynthetic uptake of nitrogen species during the early Spring; (2) the high Spring discharge rates that transport fresher water (salinities are also low), high in NO_3^- , to the lower reaches of the Estuary; and (3) the upwelling favorable winds at the mouth of Delaware Bay that lead to extremely low tides in the Murderkill Estuary. Interestingly, the two peaks in salinity and NO_3^- in each tidal period are more comparable in concentration than at any other sampling period. This would further suggest that less significant fractions of NO_3^- are being reduced during infiltration/exfiltration of tidal water than at other times of the year, consistent with the low tidal heights.

The May 2008 (MKD) sampling took place at the end of the Mother's Day Storm of 2008 (<http://www.erh.noaa.gov/phi/storms/05132008.html>). Tide levels and salinity remained high during the entire sampling period and tide levels were high enough that the whole marsh was flooded at high tide and cross-basin transfer of water and dissolved material was likely. NO_3^- levels at the sampling site remained consistently low except for short periods at flood tide due to continuing drainage of storm water from the previous days of rain and from the intense tidal flooding. Only at the very end of the sampling period, did the tidal height, discharge, and salinity patterns begin to return to normal. During the storm-dominated early part of this sampling period, DON and TDN concentrations are elevated both during the low salinity flooding period and during ebb tide. This would suggest that the composition of the entire Murderkill Estuary was affected by the addition of DON-rich waters originating from marshes along the whole Estuary.

In August 2008 (MKE), the concentrations of dissolved nitrogen species show patterns similar to those observed in July and October 2007 (MKA and MKB), although concentrations are consistently lower. The waters entering and leaving the marsh are dominated by high salinity, low nitrogen Delaware Bay water. However, NH_4^+ -rich waters are observed at the end of the ebb-tide and at the beginning of flood tide, indicating that the waters of the whole Estuary are receiving dissolved nitrogen from marsh sources. Low dissolved N concentrations may also be the result of low inputs from the watershed, due to uptake in ponds prior to discharge to the Estuary, as well as generally lower summer discharges from the watershed.

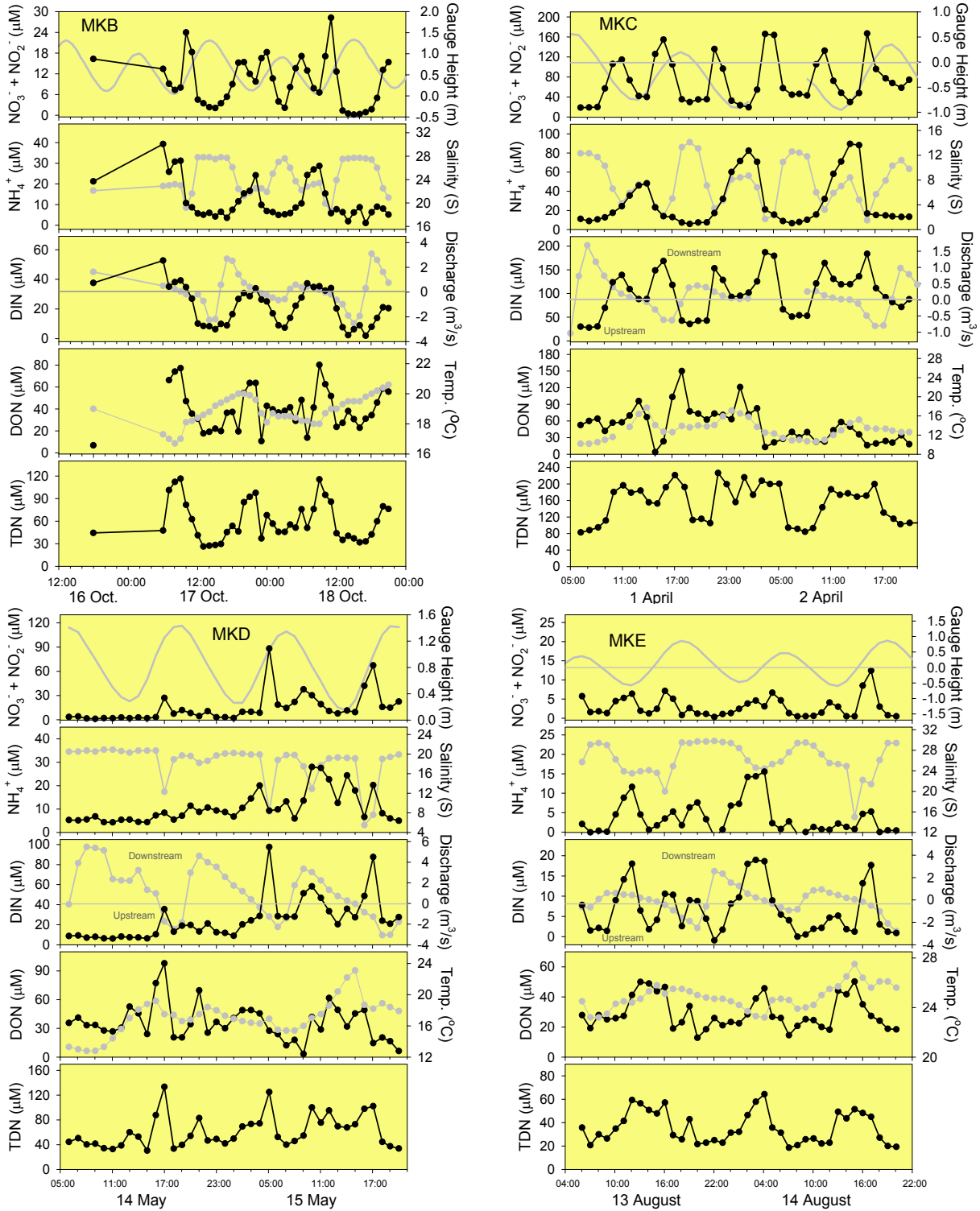


Figure 9. The distribution of dissolved nitrogen species during the MKB, MKC, MKD, and MKE sampling periods for comparison with Figure 4 showing the same parameters during the MKA sampling.

Figure 10 shows the concentrations of dissolved organic carbon (DOC), suspended solids, and particulate organic carbon and nitrogen during the MKB, MKC, MKD, and MKE sampling periods for comparison with the patterns seen during the MKA sampling period (Figure 5). Dissolved organic carbon (DOC) shows the same pattern on every sampling date, with one principal peak in concentration on each tidal cycle at the end of ebb tide, consistent with the observed pattern of NH_4^+ and Si. As in the cases of NH_4^+ and Si, this pattern suggests a primarily diagenetic source of DOC, fed presumably from the decomposition of marsh-plant detritus and peats in marsh sediments. Suspended solids, POC and PON all show patterns consistent with resuspension of material from the channel floor with peaks during both flood and ebb tides when water velocities are highest (velocity data not shown). Both fine and coarse material are suspended by channel flow, but the concentrations of fine particles are consistently much greater than the concentrations of coarse particles, most likely due much higher settling rates for coarse particles vs. fine particles and perhaps to difficulties in suspending the coarser materials from the channel floor or in entraining coarse particles from the marsh top surfaces. Although suspended sediment concentrations were high during both inflow and outflow periods during MKA and MKE, for MKB suspended sediments were most concentrated during outflow, whereas for MKC suspended sediment concentrations were most concentrated during inflows. In general, suspended sediment concentrations were highest during early spring conditions (MKC) and were lowest during late summer and autumn (MKE and MKB respectively).

The POC/PON ratios were consistently different between fine and coarse particles. In almost all cases, the C/N ratio in the coarse material is higher than for the fine material, consistent with a terrestrial or marsh vascular plant source for the coarse material. During two sampling periods (MKB and MKC), the coarse material alternates between a more marine composition and a more terrestrial composition. During the MKB (October, 2007) sampling, the coarse particles have a more terrestrial composition during the rising tide, consistent with the transport of terrestrial plant debris to the Estuary from the watershed during leaf-fall and plant senescence. During MKC (April, 2008), the terrestrial composition of the coarse material is associated with both high and low tides and may reflect either sediment erosion or enhanced transport from further up the Estuary, during this period of very low tides and salinities.

Figure 11 shows organic matter stable isotopes and elemental compositions during the MKB, MKC, MKD, and MKE sampling periods for comparison with the patterns seen during the MKA sampling period (Figure 6). Although the range $\delta^{13}\text{C}$ of DOC was -14‰ to -22‰ for all sampling periods except MKD, most periods did not show consistently maximum values at the end of ebb tide, as they did for MKA. Values of $\delta^{13}\text{C}$ of DOC for MKD were very enriched (as high as -11‰) in the first day, when the marsh was completely inundated. CPOM continued to show similar temporal patterns in $\delta^{13}\text{C}$ signatures compared to DOM, but over a smaller range - 18‰ to -21‰ . For MKA, FPOM observed during all periods had a $\delta^{13}\text{C}$ signature that was more depleted than either DOM or CPOM, ranging from -26‰ to -20‰ . FPOM often, but not always, showed its most depleted $\delta^{13}\text{C}$ signatures during mid-tides when velocities were highest – a pattern that is most clearly seen during MKE. As described for MKA, $\delta^{13}\text{C}$ signatures of possible end-members include: (1) warm-climate terrestrial grasses, including *Spartina spp.*, that use the C-4 photosynthetic pathway and have $\delta^{13}\text{C}$ of -12‰ to -14‰ ; (2) marine and estuarine algae that have $\delta^{13}\text{C}$ of about -20‰ ; and (3) most other terrestrial plants, including all

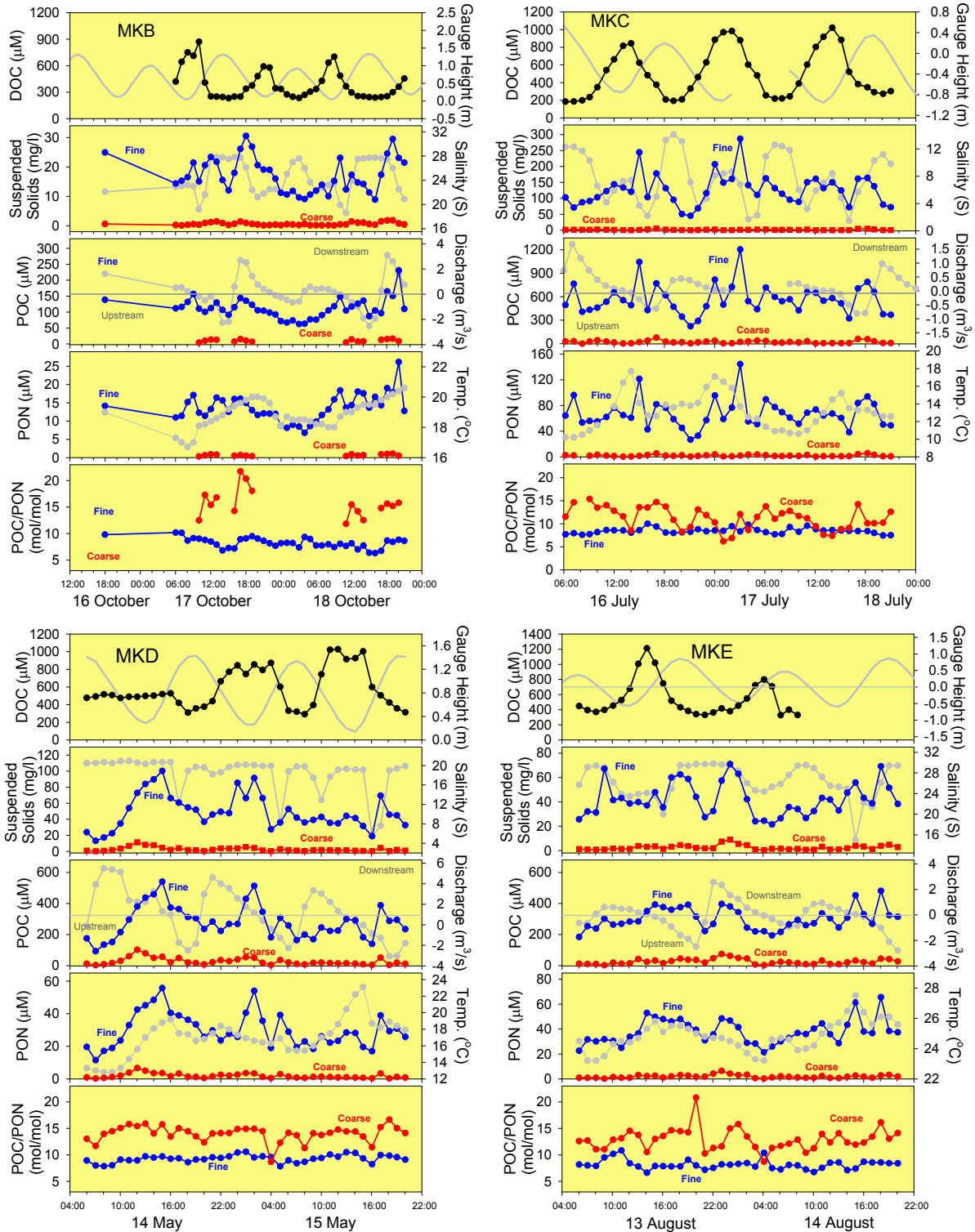


Figure 10. The concentrations of dissolved organic carbon (DOC), suspended solids, particulate organic carbon (POC) and nitrogen (PON) in both the fine (0.45-63 μm) and coarse (63-2000 μm) size fractions during the MKB, MKC, MKD, and MKE sampling periods for comparison with Figure 5 showing the same parameters during the MKA sampling. Gauge height, salinity, discharge, and temperature data are shown in light gray.

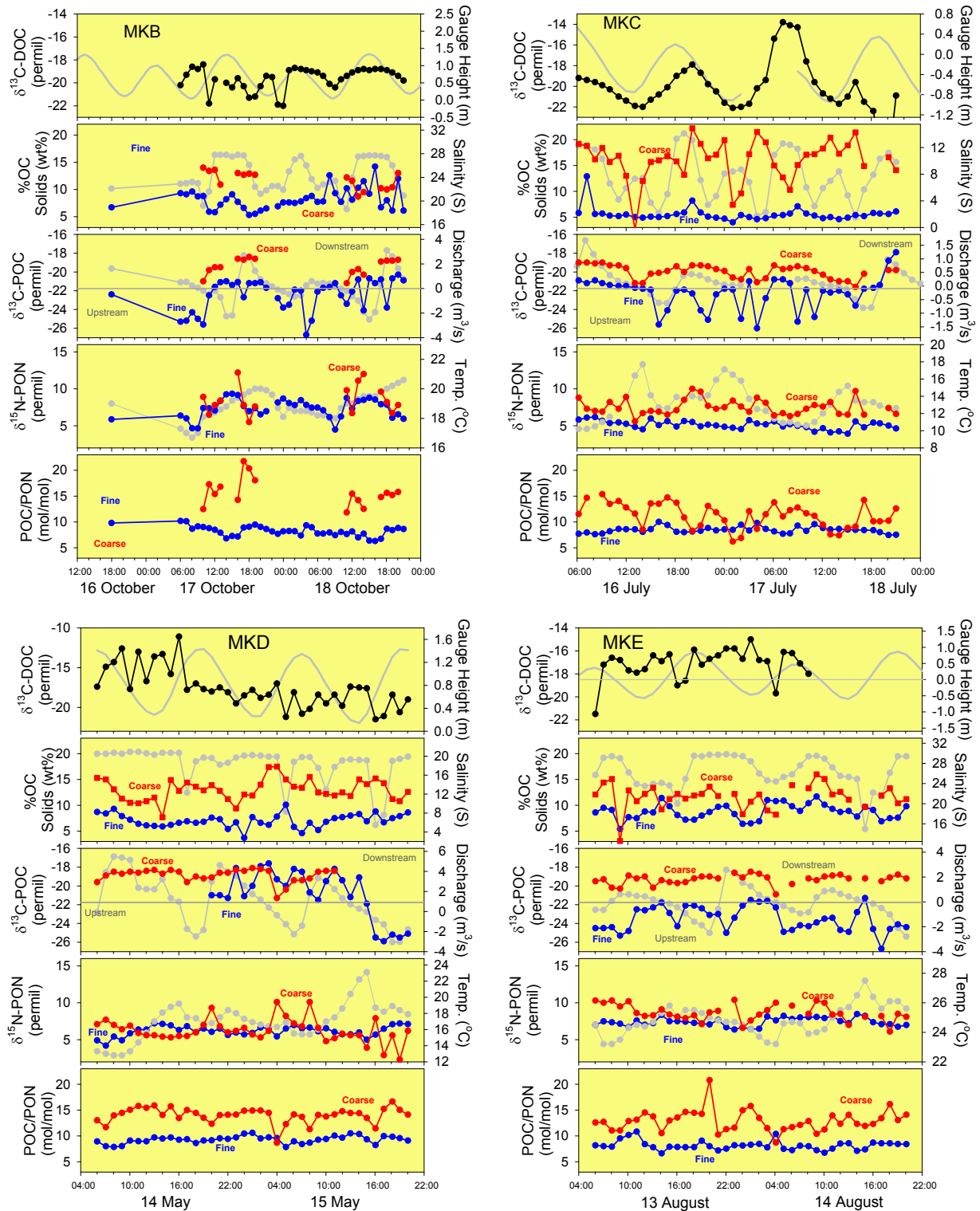


Figure 11. Elemental and isotopic composition of dissolved and particulate organic matter during the MKB, MKC, MKD, and MKE sampling periods for comparison with Figure 6 showing the same parameters during the MKA sampling. Gauge height, salinity, discharge, and temperature data are shown in light gray.

broad leaves and cool-season grasses, that use the C-3 photosynthetic pathway and have $\delta^{13}\text{C}$ of -27‰ to -28‰. Therefore, DOC and CPOC both have clear contribution from C-4 grasses and FPOC has a clear contribution from C-3 plants, most probably from upland soils. However, one isotope cannot be used with three end-member sources for either exact quantification of carbon contribution from each or exclusion of one. Weight percent carbon and C/N ratio both suggest that CPOM is primarily composed of moderately degraded leaf detritus, whereas FPOM is likely highly processed organic matter that is more tightly associated with minerals (Aufdenkampe et al., 2007). Thus, fine vs. coarse suspended sediment fractions appear to have contrasting sources and history, whereas DOM and CPOM both appear to have similarly substantial contributions from salt marsh grasses such as *Spartina spp.*

Figure 12 shows dissolved gas concentrations and some related parameters during the MKB, MKC, MKD, and MKE sampling periods for comparison with the patterns seen during the MKA sampling period (Figure 7). Dissolved oxygen concentrations were highly variable over each sampling period, with concentrations typically dropping down to 1-3 mg/L at the end of ebb tide. DO increased dramatically each rising and flood tide, approaching and sometimes exceeding saturation values with respect to equilibrium with the atmosphere. The most notable oversaturation occurred during MKE at the very end of ebb tide but only during daytime. The same outflow conditions at night during MKE showed a sharp drop in DO to nearly 1 mg/L. Dissolved free CO_2 concentrations, represented as the partial pressure of pCO_2 , nearly always reflected a mirror image pattern with DO concentrations. The peaks in pCO_2 were buffered downward by co-occurring increases in total alkalinity; otherwise pCO_2 would be higher. Alkalinity pulses during late ebb tide are only absent during the first half of MKD, when storm waters were still draining over the surface of the marsh rather than driving discharge of pore water. For MKB and the first half of MKC, we have $\delta^{13}\text{C}$ data for dissolved inorganic carbon (DIC, the sum dissolved CO_2 , HCO_3^- & CO_3^{2-}), before our TIC-TOC instrument began its multi-year saga of malfunctions. This data shows a clear pattern of lower $\delta^{13}\text{C}$ when DIC concentrations spike, showing that respiration of organic matter is the source of elevated CO_2 , although it is not possible to distinguish between organic matter sources because all are significantly depleted in ^{13}C relative to the atmosphere.

Figure 13 shows the distribution of SRP ($\approx \Sigma\text{PO}_4^{3-}$) and dissolved silicate (Si) during the MKB, MKC, MKD, and MKE sampling periods. In contrast to the MKA (July 2007) sampling period, where SRP concentrations peaked during both ebb and flood periods with high flow velocities and with high suspended sediment concentrations, SRP during MKB, MKC, MKD, and MKE sampling periods only show one peak in concentration per tidal cycle. This would suggest that the mechanism of SRP addition is different in these latter sampling periods than during the MKA. In MKA, the SRP concentration peaked during inflow of low salinity water from the Estuary and then again as those waters discharged from to the marsh channel at falling tide, and SRP seemed to momentarily decline during the peak in DOC, NH_4^+ and Si at the low ebb tide. In MKB and MKE, on the other hand, SRP peaks coincided with DOC, NH_4^+ and Si peaks at the low change of tides and lowest salinities (Figures 9, 10 and 13). During MKC, the SRP

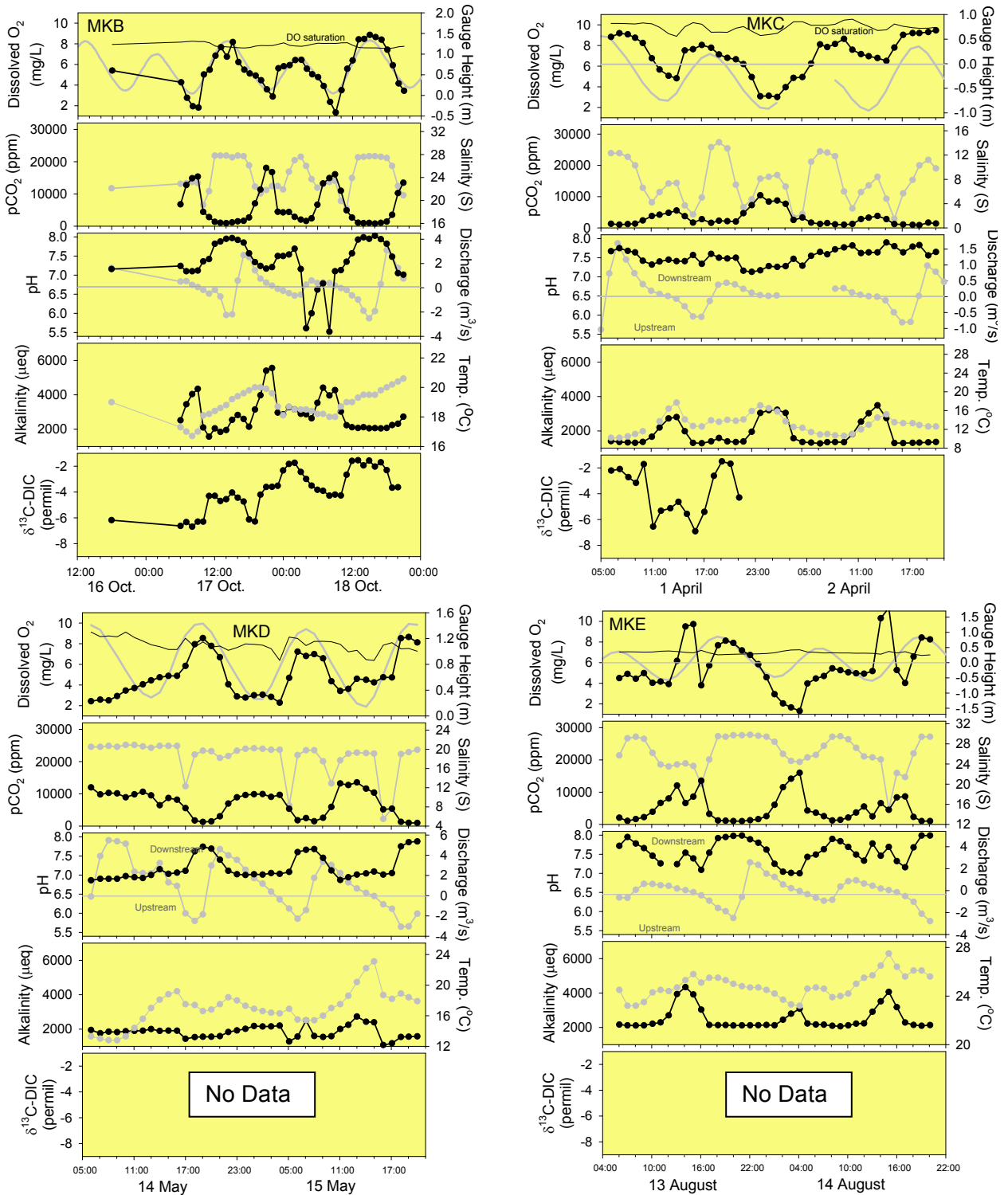


Figure 12. Dissolved O₂, the partial pressure of dissolved free CO₂ (pCO₂), pH, total alkalinity and δ¹³C of dissolved inorganic carbon (DIC, where measured) during the MKB, MKC, MKD, and MKE sampling periods for comparison with Figure 7 showing the same parameters during the MKA sampling. δ¹³C of DIC was not measured where values are not shown. DO saturation is indicated by the thin black line and varies as a function of both temperature and salinity. Gauge height, salinity, discharge, and temperature data are shown in light gray.

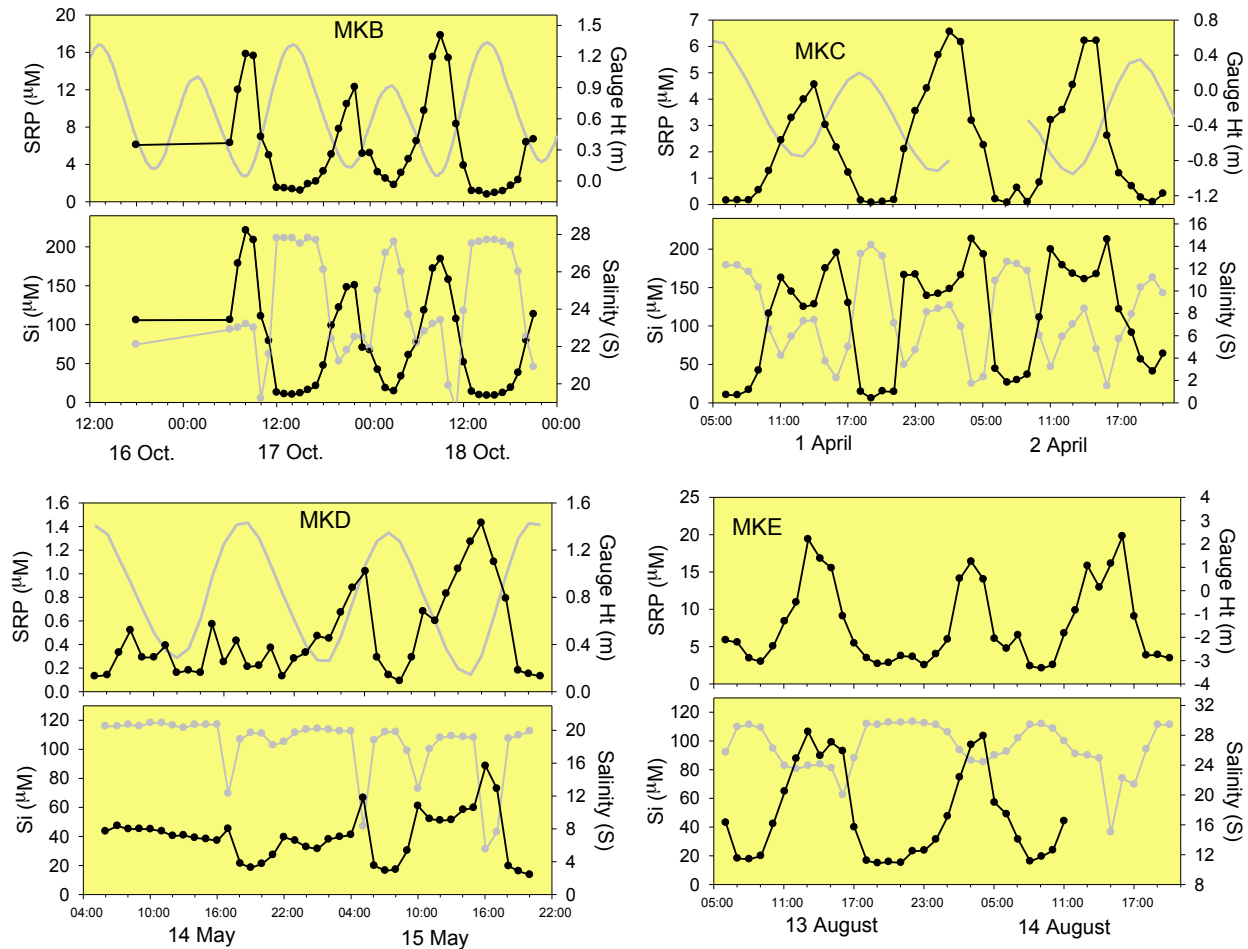


Figure 13. The distribution of soluble reactive phosphorus ($\text{SRP} \approx \Sigma \text{PO}_4^{3-}$) during the MKB, MKC, MKD, and MKE sampling periods for comparison with the MKA period (Figure 8). Gauge height, salinity are shown in light gray.

peak coincided at low tides with high DOC, but Si and salinity showed a local minimum and maximum at those times. For MKD, SRP peaked during the rising tide when salinity was at its minimum but also when DOC and suspended solids are high. In all cases it appears that SRP is highest in lower salinity waters, but that the salt marsh may have also served as an SRP source in all periods except MKA.

Dissolved Si appears to be controlled by low tide resuspension during the MKA, MKB, MKD and MKE sampling periods (single concentration peak at low tide). During the consistently low tide of the MKC sampling period, however, Si appears to have two minor peaks that depend inversely on salinity, consistent with an estuarine source followed by drainage of these source waters from channel banks at falling tide.

Taken together, SRP and Si appear to have three sources in Webbs Marsh waters: (1) from the fresher waters of the Murderkill Estuary; (2) from porewater discharge (some of which may have initially come from recharge by fresher waters of the Murderkill Estuary on the previous flood tide; and (3) from resuspension/desorption. The relative importance of these sources and the processes contributing to source intensity apparently varies through the seasons.

4.4 Analysis of Loads: Failure of the Conventional Approach

Our observations of temporal patterns in nutrient species' concentrations and composition suggest that Webbs Marsh consistently served as a source for some dissolved species (i.e. DOC, DON, NH_4^+ , Si, Alkalinity, CO_2) and a sink for others (i.e. DO). However, qualitative analysis does not provide a clear view into the net fluxes of many dissolved species and most particulate species. Quantitative analysis of net fluxes, or loads, is required to not only distinguish more subtle patterns but also to guide quantitative computer models for the Murderkill Estuary.

Our initial plan was to sum up hourly loads based on the product of discharge and the concentrations of measured parameters to determine a tidal or daily average loads for each parameter:

$$J_s = \sum_{i=1}^n C_{ms}^i \times Q_i \quad (1)$$

where, Q_i is the discharge measured over some interval of time with positive values representing discharge out of the marsh and negative values representing water fluxes into the marsh, C_{ms}^i is the measured concentration of some species, s , over the interval of time for which Q_i was determined, and J_s represents summed load for the time period of interests (a number of hours, n , representing a day or tidal period).

Figure 14 shows the temporal patterns that result from instantaneous loads calculated using equation 1 for DIN (dissolved inorganic nitrogen = $\text{NO}_3^- + \text{NH}_4^+$), DON (dissolved organic nitrogen = TDN – DIN), TDN (total dissolved nitrogen), SRP and Si during MKA sampling period (July 2007). This figure also serves as an example of problems with this approach for calculating loads over periods longer than the sampling interval of 1 hour. First, the instantaneous hourly loads calculated in this manner have a temporal pattern that is nearly always identical to discharge (Figure 14, grey plot in middle panel) despite rather different temporal patterns in concentrations of DON vs. SRP vs. Si for example (Figures 4 and 8). This is because in a tidal system discharge has a much larger dynamic range than nutrient species concentrations. Second, with water discharge changing direction and sign every 4-7 hours, Equation 1 effectively amounts to calculating the relatively small difference between large inflow and large outflow loads (i.e. $\Sigma(\text{ebb loads}) \approx \Sigma(\text{flood loads})$). Thus, the propagation of summed errors over that difference amplifies the relative errors in the calculated net loads, such that net loads were only rarely significantly different from zero.

Although the uncertainty can be somewhat reduced by calculating and reporting diurnal loads from the average of a running average of loads for a 25 hour period (close to twice the major semi-diurnal tide period of 24.84 hours that would average over two tidal cycles to reduce the effect of the diurnal inequality), the uncertainties remain high compared to the summed loads. Last, any imbalance in water fluxes during the 25-hour tidal period will directly and proportionally lead to a systematic biasing of all net nutrient loads for a given period. Although Webbs Marsh was selected because of its well-constrained tidal flows through a single channel, water fluxes were not in perfect balance. Water fluxes out of the marsh were larger than water fluxes into the marsh by +4.4%, +28.7%, +25.0%, +318% and +6.3% for MKA, MKB, MKC, MKD and MKE respectively. Any species flux calculated by Equation 1 would have the same positive load biases. Salt imbalances were very similar to water imbalances – +7.0%, +29.0%, +55.9%, +383%, +7.6% larger outfluxes than influxes – suggesting that the unmeasured water flowing into the marsh was of similar salinity to the measured water fluxes into the marsh.

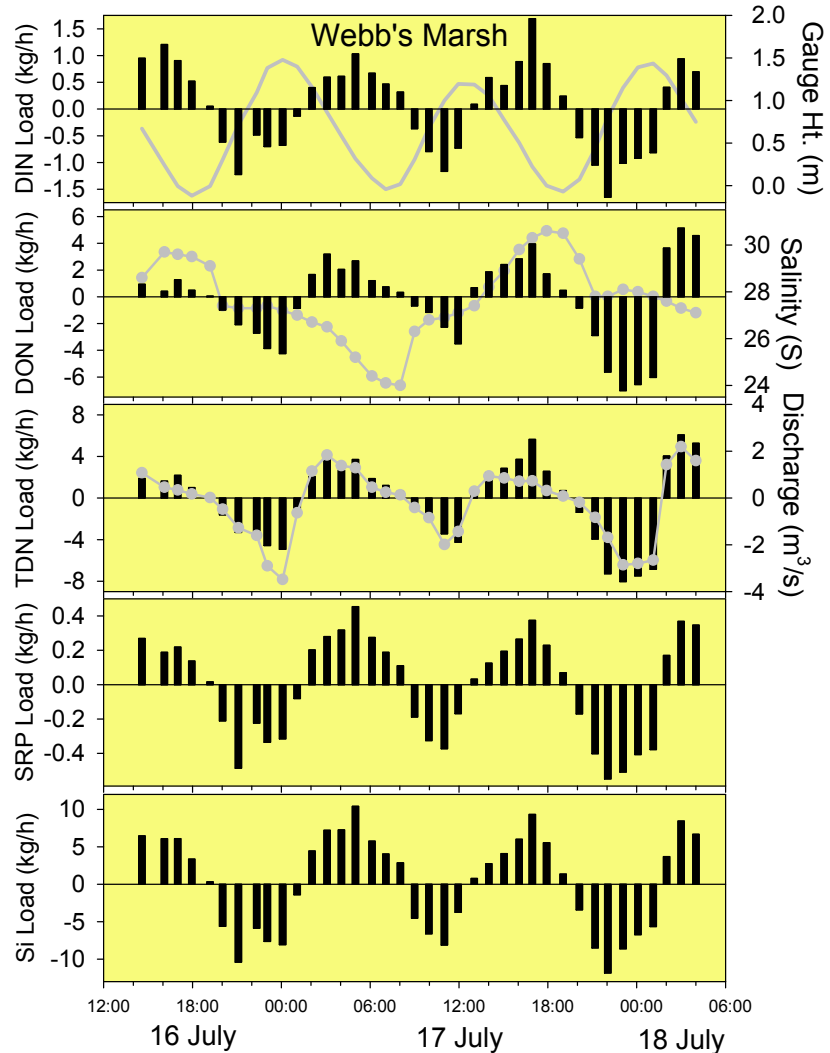


Figure 14. Instantaneous loads determined on the hour from Webbs Marsh to the Murderkill Estuary during the MKA sampling period (July 2007). These loads were calculated from the concentrations and discharges determine on the hour at the Webbs Marsh gauging station. Gauge height, salinity and discharge are shown in light gray.

4.5 Concentrations as a Function of Salinity: Evaluation of Conservative Mixing

An alternative approach had to be developed to overcome the problems of using the conventional approach to calculating loads from rivers on a tidal system. We framed the alternative approach on the classic estuarine science concept of examining a property relative to variations in salinity. Because salt mixes conservatively, it can be used as an index to track the relative proportions two end-member waters in a mixture. Plots of a property as a function of salinity can thus reveal if that property also behaves conservatively and “falls along the conservative mixing line,” or whether there is a potential net source (“addition”) or sink (“removal”) for that property within the mixing zone (Figure 15).

We were able to effectively use this approach because of the high mixing rates in the Murderkill Estuary between waters from the freshwater Murderkill River and the saline Delaware Bay (deWitt and Daiber, 1974). This mixing occurred over timescales that were much faster than nutrient production or consumption fluxes in the Estuary. Thus, most of the parameters of interest appeared to be conservative over tidal timescales in the Murderkill Estuary (i.e. linearly dependent on conservative salinity) and most of the biogeochemical species entering Webbs Marsh reflect conservative mixing between the freshwater Murderkill River and the saline Delaware Bay. This allowed us to assess the effect of biogeochemical production and consumption of these parameters within the marsh by investigating parameter vs. salinity diagrams, where inflow waters fall on a linear mixing line and deviations from this line in outflow waters reflect sources or sinks due to processes within the marsh. These deviations were typically most apparent toward the end of each ebb tide when water levels were lowest.

Figure 16 shows parameter vs. salinity plots for the MKA sampling period (July 2007). The patterns are clear and consistent for dissolved species likely originating from marsh sediment pore waters (i.e. NH_4^+ , DOC, and Si). Waters flowing into Webbs Marsh (shown with blue symbols, with darker shading for higher water flows) had NH_4^+ , DOC, and Si concentrations that were linear with salinity as the Murderkill River end member mixes with higher salinity Delaware Bay waters. All three inflow periods during MKA (hours 6-9, 20-22 & 31-34) showed nearly identical relationships with salinity for these three parameters. Note that for the first 1-2 hours after flow reversal, inflowing water chemistry typically looks similar to what had just previously flowed out of the marsh. We have thus ignored these early inflowing waters with respect to defining inflow mixing lines. Waters flowing out of Webbs Marsh had NH_4^+ , DOC, and Si concentrations that clearly fell above this inflow line, indicating a strong source within the marsh that cannot be accounted for by simple mixing of inflow waters (Figure 16).

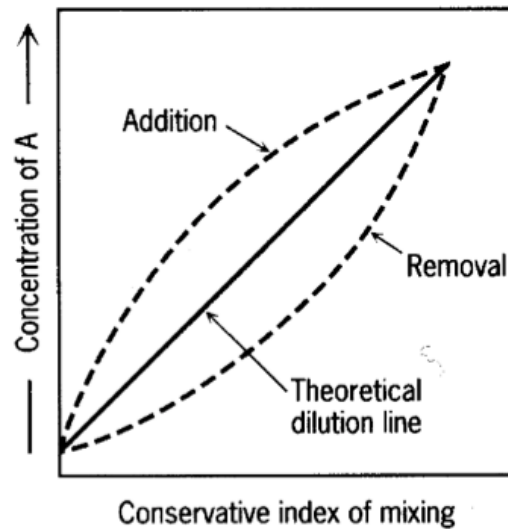


Figure 15. The graphical approach to determining net source or sink of a species within a mixing zone by using a conservative index such as salinity.

Other species shown in Figure 16 have more complicated patterns. NO_3^- exhibited high river end member concentrations and two distinct inflow mixing lines. Dissolved oxygen (DO) also fell along two different lines, with the two afternoon low-low tides at hours 6-9 and 31-34 falling on the same line. Differences and similarities are meaningful in the slopes and intercepts of these inflow mixing lines. In the case of DO, the daytime inflow waters reflect planktonic oxygen production in both the Bay and River end member waters. All outflow waters from MKA

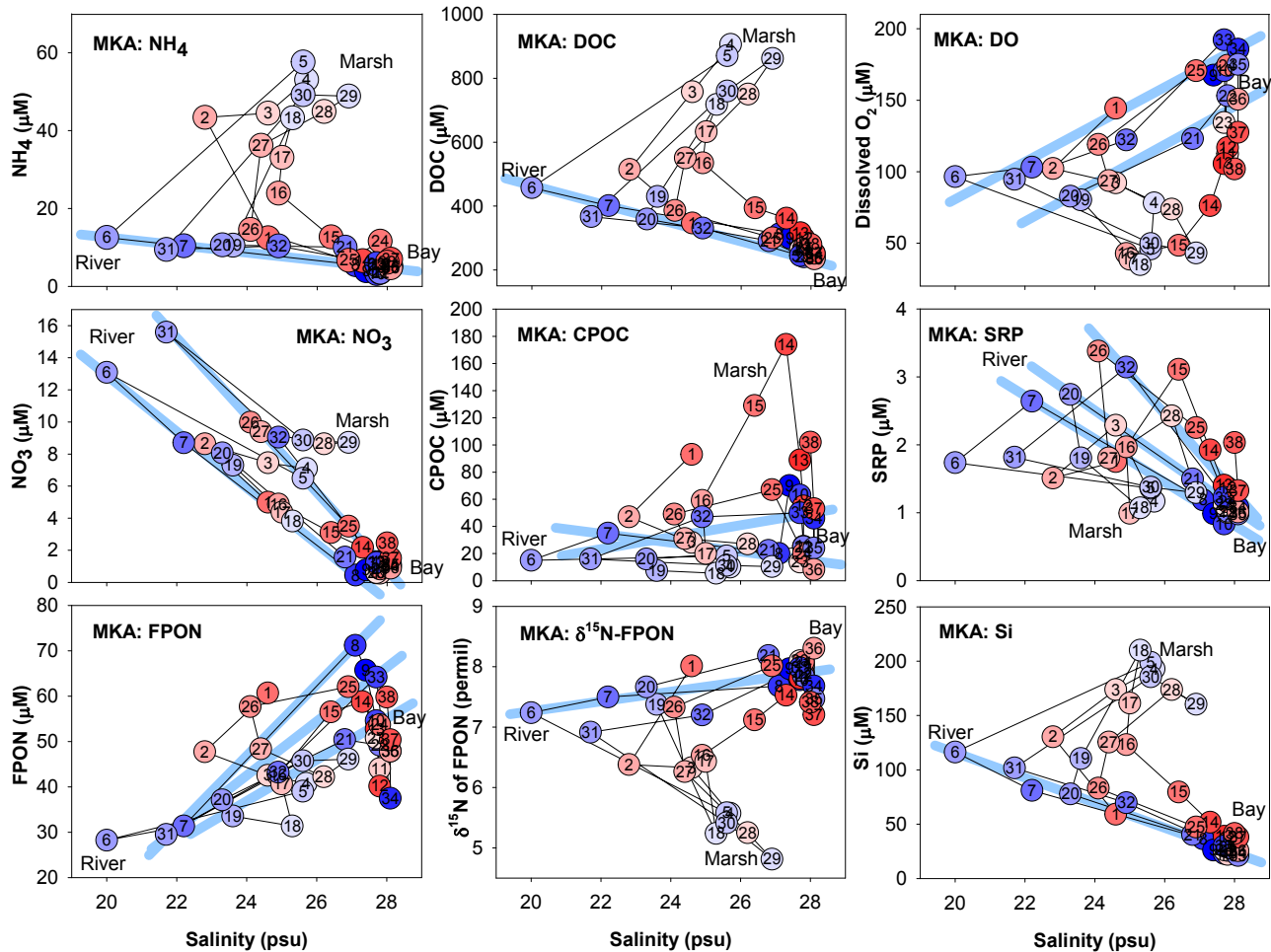


Figure 16. Selected bioactive species from MKA plotted as a function of salinity. Blue symbols indicate inflow to the Marsh and red outflows, with shading intensity proportional to discharge. Numbers within symbols designate the sampling hour. Pale blue lines represent conservative mixing lines during each flood tide between of Murderkill River and Delaware Bay end members.

had lower DO concentrations than would be expected from the immediately preceding inflow based on salinity. This is a clear indication that the marsh consumed DO. Particle associated species – such as FPON, CPOC and, in this case, SRP – typically had the most complicated relationships because concentrations reflected not only mixing between Bay and River but also resuspension from within the tidal channel at mid flood tide when water velocities were highest. Despite the challenge in distinguishing whether the marsh is a net source or sink of FPON based on concentrations, its $\delta^{15}\text{N}$ clearly shows that the FPON leaving the marsh has a distinct signature consistent with marsh vegetation.

Figure 17 shows parameter vs. salinity plots for the MKB sampling period (Oct. 2007). Patterns were very similar to those observed for MKA. One notable exception was that CPOC inflow “lines” showed significant upward curvature, indicating a potential source within the Murderkill Estuary mixing zone, with Webbs Marsh acting as a source or sink depending on the tidal cycle.

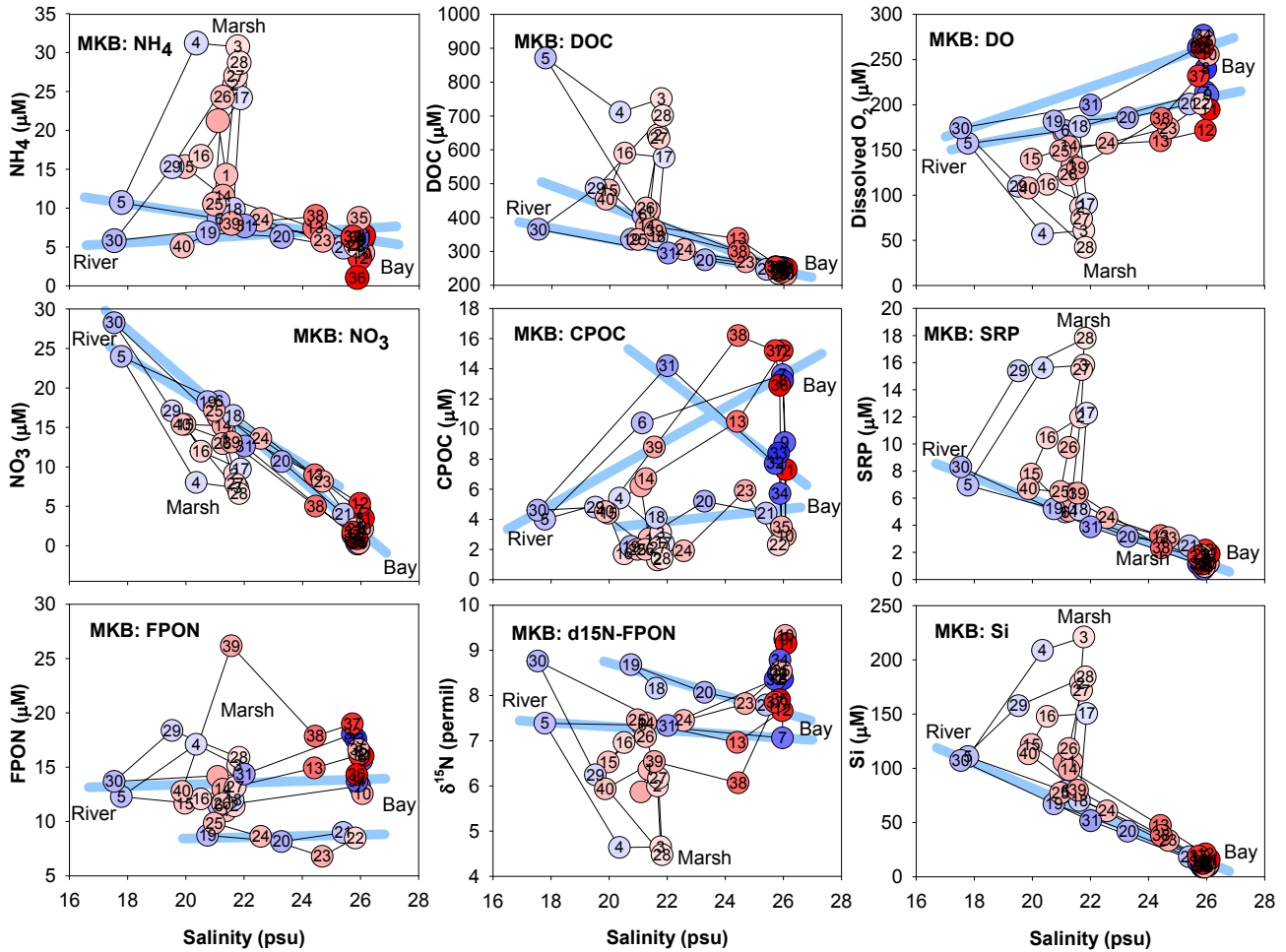


Figure 17. Selected bioactive species from MKB plotted as a function of salinity. Symbols and lines are as in Figure 16.

Figure 18 shows parameter vs. salinity plots for the MKC sampling period (April 2008), which occurred during very low water levels due to prevailing winds blowing tides offshore. Patterns were similar to those observed for MKA & MKB. Three exceptions include the marsh being a sink for nitrate, the upward curvature of the mixing line for FPON, and the moderate Marsh source of Si in contrast to the stronger Marsh sources seen earlier.

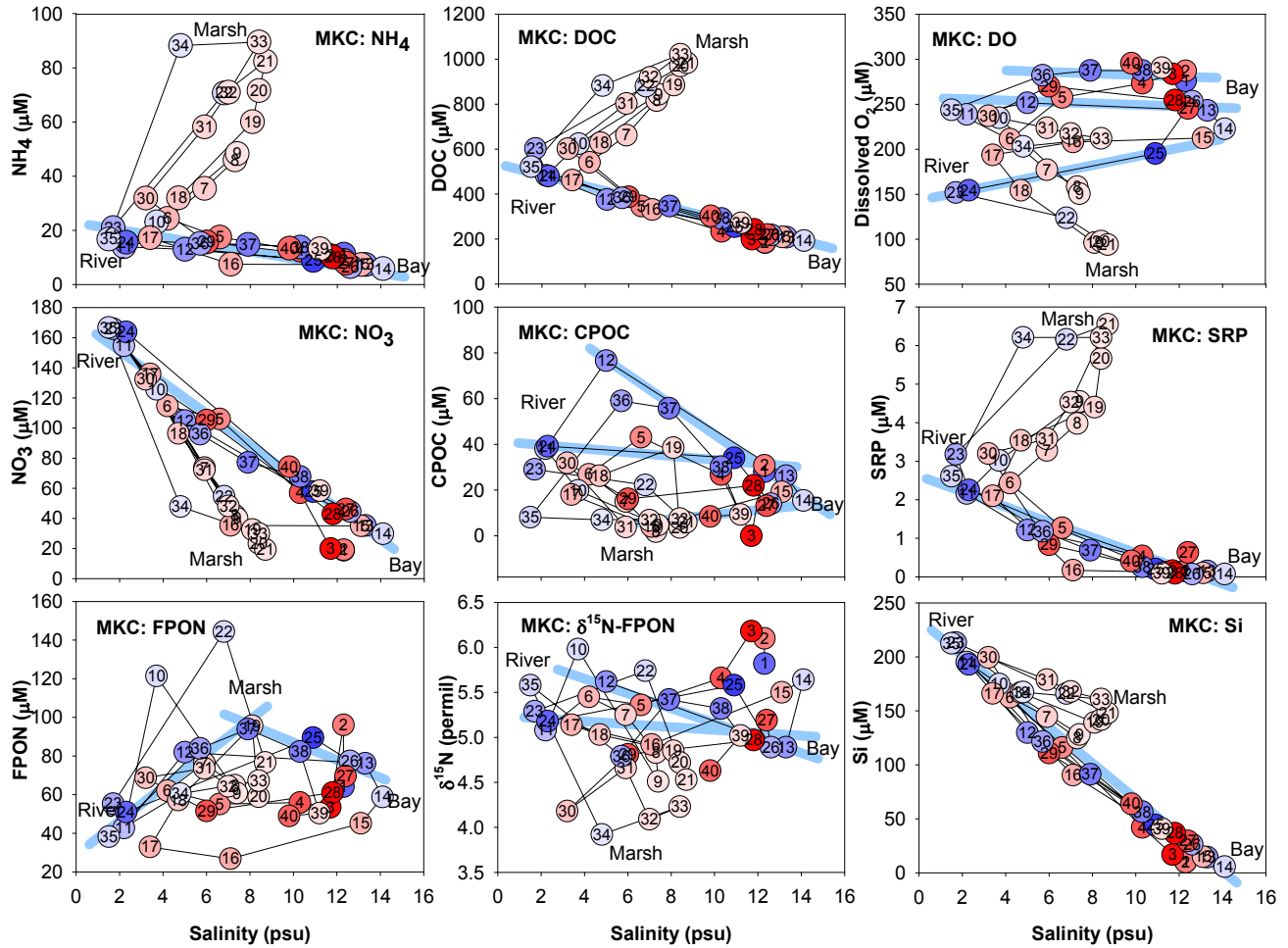


Figure 18. Selected bioactive species from MKC plotted as a function of salinity. Symbols and lines are as in Figure 16.

Figure 19 shows parameter vs. salinity plots for the MKD sampling period (May 2008), which occurred as waters receded following the “Mother’s Day” storm. This was a period of exceptionally high water levels and nearly continuous discharge of saline floodwaters from the marsh with large associated export fluxes. Despite this, general patterns were similar to previous sampling periods.

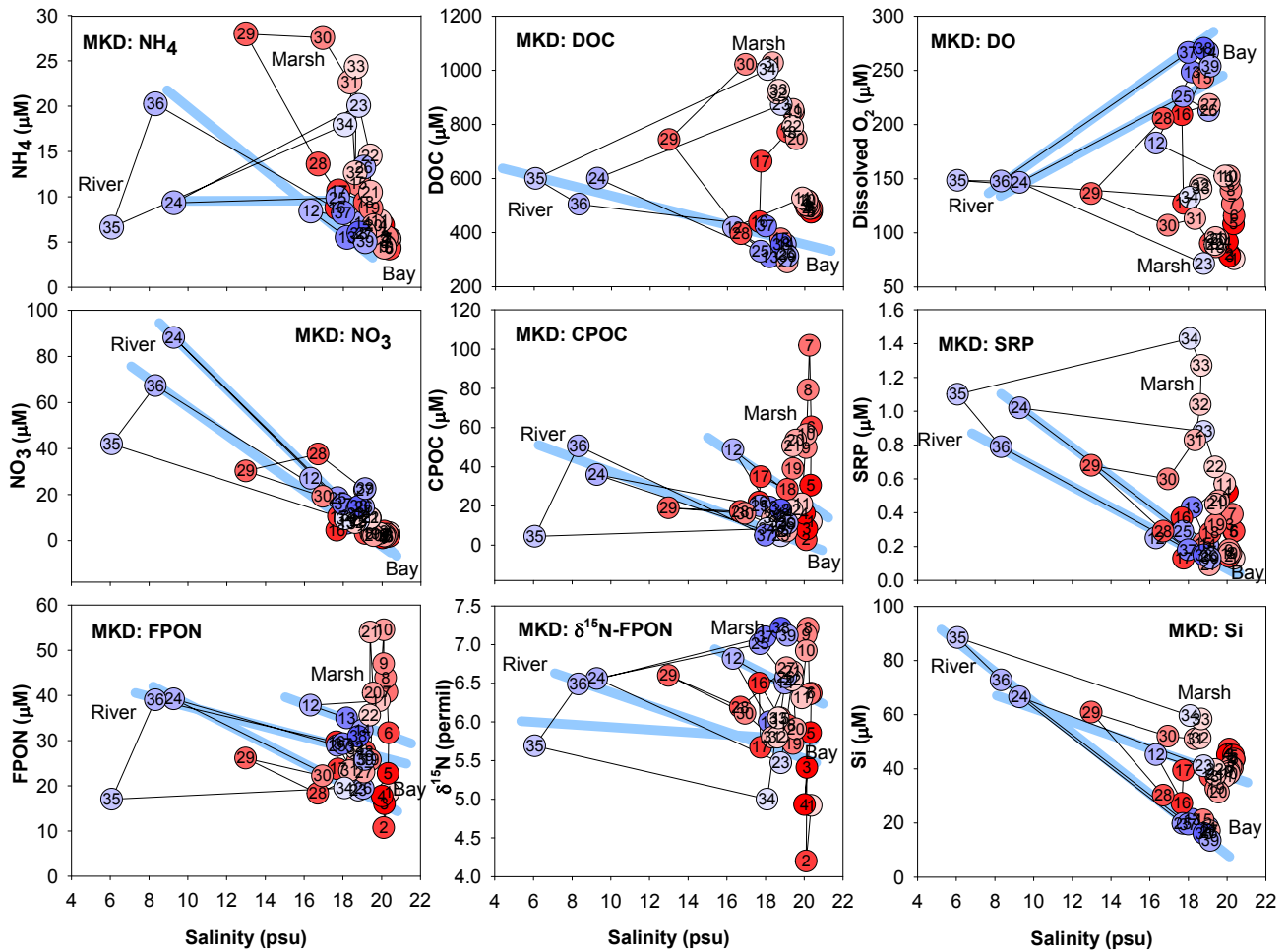


Figure 19. Selected bioactive species from MKD plotted as a function of salinity. Symbols and lines as in Figure 16.

Figure 20 shows parameter vs. salinity plots for the MKE sampling period (Aug. 2008). Patterns were similar to those observed previously. One exception is the observation that the Marsh appears to produce and export excess dissolved oxygen for two short afternoon periods (see Figure 12).

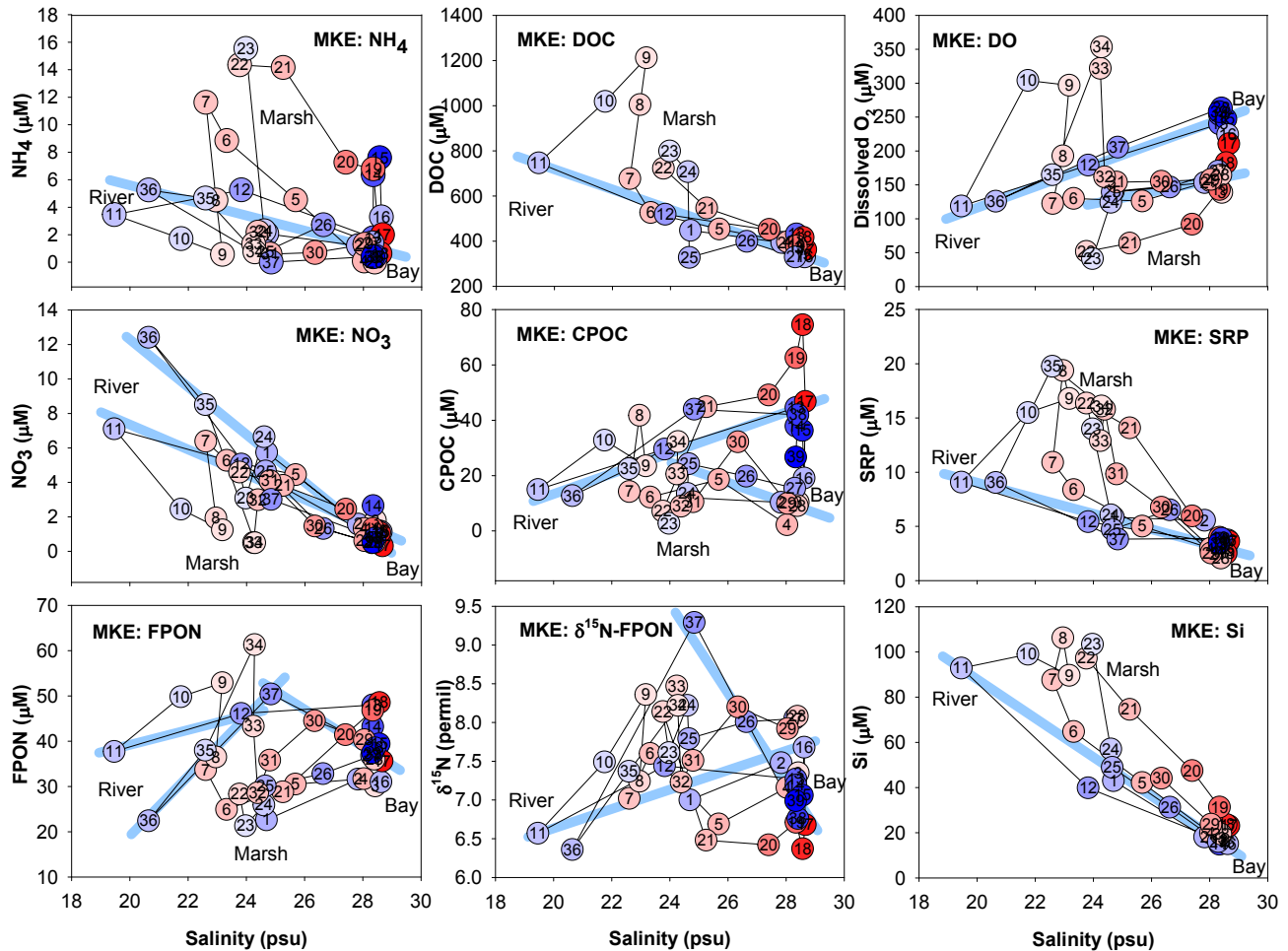


Figure 20. Selected bioactive species from MKE plotted as a function of salinity. Symbols and lines are as in Figure 16.

4.6 Analysis of Loads: Novel Approach Using Anomalies to Conservative Mixing

Our approach to calculating net fluxes, or loads, of biogeochemically active species in or out of Webbs Marsh relies on a quantitative evaluation of anomalies to conservative mixing. We can use statistical regression analysis of species concentrations as a function of salinities at each hour water flows into Webbs Marsh to assess the degree to which each species reflects conservative mixing between the freshwater Murderkill River and the saline Delaware Bay. We can then use this regression equation to calculate the predicted species concentration at each hour based on the salinity. Thus the difference between predicted versus measured concentrations of the given species gives us a quantitative estimate of the anomaly, and is

functionally equivalent to calculating the difference between inflow and outflow for each sampled hour. For the hours that are used to develop the regression, in which waters are flowing into Webbs Marsh, these anomalies are equivalent to regression residuals and are typically close to zero. For hours in which waters are flowing out of Webbs Marsh the anomalies can be quite large, especially toward the end of each ebb tide when water levels were lowest (Figures 16-20).

These species concentration anomalies can be multiplied to by discharge to calculate loads:

$$J_s = \sum_{i=1}^n (C_{ps}^i - C_{ms}^i) \times Q_i \quad (2)$$

where, C_{ps}^i represents the predicted concentration from conservative mixing of a species (s) for the given salinity, and as with equation 1, C_{ms}^i is the measured concentration of the same species, Q_i is the discharge measured over some interval of time, and J_s represents summed load for the time period of interest.

The advantage of this procedure is that the predicted and measured concentrations during at least half of each tidal cycle are nearly the same. The key difference with the traditional approach given in Equation 1 is that in Equation 2 the difference in outflow vs. predicted inflow concentrations at each hourly sampling interval is calculated before multiplying by discharge. This has the effect of multiplying all the inflow discharges by concentration anomalies ($C_{ps}^i - C_{ms}^i$) that are negligible (≈ 0). Thus, inflows will neither contribute to the summed load in or out of the marsh nor to the associated propagation of error. Only the loads where there is significant deviation between measured and estimated concentrations contribute significantly to net loads. Also, with inflow discharges being nearly zeroed out by negligible concentration anomalies, net species fluxes are effectively based on outflow discharges alone and are no longer biased by issues with net water imbalance.

As can be seen in Figures 16 to 20, a separate mixing curve must be calculated for each tidal cycle to take into account the changing compositions of the end-members waters that mix to yield the composition of Murderkill Estuary water that floods Webbs Marsh. On most occasions, the composition of the Delaware Bay end-member (salinity and parameter concentration) represented the major source of variation over a single sampling period reflecting tidal processes, wind conditions, and discharge affecting mixing in Delaware Bay. Also, we often excluded from the inflow regression the first 1 to 2 hourly samples of flooding tides, as the composition of these waters indicated that these were just a return of the same waters that flowed out of the marsh 1 to 3 hours earlier (Figures 16-20). Last, because the ever changing tides in the Murderkill are dynamic enough that each 25 hour period has a unique flow distribution, we calculated and reported diurnal loads from the average of a running average of loads for each of the fifteen 25 hour intervals in each 40 hour sampling period. The standard deviation of this average net load for each species is given as the uncertainty in Tables 3 and 4, but is more accurately interpreted as temporal variability between the fifteen 25 hour intervals. Statistical significance of a net load is indicated by a relative standard error, or coefficient of variation, less than 50% (i.e. 2 times the standard error provides a 95% confidence that the net load is not equal to zero).

Tables 3 and 4 show the net loads of most measured species to the Murderkill Estuary from Webbs Marsh, and their associated uncertainties, calculated using the approach described above and the potentially flooded area of Webbs Marsh (0.64 km²; T.E. McKenna, personal communications). The marsh consistently served as source for NH₄⁺, DON, all P species, DOC, pCO₂, alkalinity and Si, and as a sink for NO₃⁻ (except MKA) and DO (except MKC, more on this later). We knew from the qualitative analysis of species vs. salinity plots that the marsh was a source of dissolved and particulate nutrients and carbon, but, as a result of our quantitative analysis we have load estimates and uncertainties that allow us to compare the magnitudes of these loads. In addition, we can multiply the net flux of reduced species by their oxidation ratio (OR; the number of moles of O₂ required to fully oxidize a mole of organic carbon; see Section 4.7) to compare the effects of material loads and oxygen deficit (the amount of oxygen needed to bring oxygen depleted marsh waters back to saturation with respect to the atmosphere) that both contribute to the biogeochemical oxygen demand in the Murderkill Estuary. Waters leaving the marsh with DO concentrations lower than those in the Estuary will have an immediate effect on DO concentrations in the Estuary, whereas oxidation rates of other materials might result in delays in their effects on estuarine oxygen demand on the order of hours (i.e. NH₄⁺) or days to months (i.e. organic matter species). Note that the oxidation ratios for dissolved organic matter (DOM), fine particulate organic matter (FPOM), and coarse particulate organic matter (CPOM) all depend on the elemental composition of the organic matter (Anderson, 1995; Hedges et al., 2002; Masiello et al., 2008; Richardson et al., 2013). This issue of what oxidation ratio value to use for organic matter exported from salt marshes or in estuarine sediments has important implications to properly modeling and estimating the dissolved oxygen in the Estuary. A discussion of these values is given in section 4.7, below.

In Tables 3 and 4, we see that despite some consistent patterns for some species between sampling periods, there were also strong differences between sampling periods for other species.

During MKA (July 2007) the marsh was a clear and statistically significant sink for dissolved oxygen and for Chlorophyll *a* and a significant source for NO₃⁻, NH₄⁺, DON, CPON, PO₄³⁻, TDP, DOC, CPOC, CO₂, alkalinity, Si and CSS (Tables 3-4). Net loads for fine suspended sediments (FSS) and associated carbon (FPOC), nitrogen (FPON) and phosphorus (PP) were not statistically significant. CPOM had the largest net effect on the Murderkill Estuary oxygen demand; despite the relatively low concentrations of CPOM, its relatively large positive concentration anomalies were timed to correspond exactly with the largest water discharge fluxes from the marsh. Oxygen demand from DOM and DO-depleted waters were slightly lower, followed by FPOM and NH₄⁺. Together, these 5 species accounted for a total average oxygen demand for the 2-day period of 110 gO₂/m²/y (±13%) or 11,800 μmol/m²/d.

Net loads during MKB (Oct. 2007) showed a similar pattern as for MKA, but the magnitude of the loads were about 20% to 40% smaller and, as a consequence, often less statistically significant (Tables 3-4). The DO deficit load was the largest contributor to the oxygen demand exported to the Murderkill Estuary.

Table 3. Net loads to the Murderkill Estuary from Webbs Marsh (0.64 km²) in units of g/m²/y for each of our five 40-hour sampling periods, determined using our novel approach using anomalies to conservative mixing. Positive values (red) are net downstream fluxes out of the marsh, whereas negative values (blue) are net upstream into the marsh. Relative uncertainties for each species net load were calculated as described in the text, and were propagated by quadrature to uncertainties of sums and averages. MKD was excluded from the average because it followed the very large Mother's Day storm.

Mean Flux	MKA Jul Jul. 2007 g/m ² /y	MKB Oct Oct. 2007 g/m ² /y	MKC Apr Apr. 2008 g/m ² /y	MKD May May 2008 g/m ² /y	MKE Aug Aug. 2008 g/m ² /y	Average Excluding MKD g/m ² /y
Total N (g N)	5.62 ± 19%	0.52 ± 187%	-3.68 ± 41%	13.55 ± 44%	2.30 ± 45%	1.19 ± 195%
NO ₃ ⁻ + NO ₂ ⁻	0.40 ± 13%	-0.05 ± 92%	-2.33 ± 28%	-4.70 ± 19%	-0.19 ± 14%	-0.54 ± 123%
NH ₄ ⁺	1.19 ± 6%	0.33 ± 40%	0.86 ± 4%	2.12 ± 130%	-0.11 ± 134%	0.57 ± 37%
DON	4.15 ± 19%	0.07 ± 1438%	2.14 ± 57%	16.95 ± 28%	1.99 ± 49%	2.09 ± 96%
FPON	-1.02 ± 69%	0.20 ± 72%	-4.13 ± 13%	-1.78 ± 103%	0.14 ± 204%	-1.20 ± 79%
CPON	0.91 ± 15%	-0.03 ± 140%	-0.22 ± 14%	0.95 ± 65%	0.47 ± 6%	0.28 ± 52%
Total P (g P)	0.62 ± 16%	0.98 ± 7%	0.23 ± 23%	1.81 ± 4%	2.53 ± 3%	1.09 ± 13%
PP, total	0.08 ± 104%	0.03 ± 114%	0.00 ± 0%	0.58 ± 56%	-0.02 ± 164%	0.03 ± 399%
PO ₄ ³⁻	0.57 ± 13%	0.51 ± 10%	0.09 ± 19%	0.13 ± 84%	1.02 ± 15%	0.55 ± 32%
TDP (PO ₄ +DOP)	0.53 ± 9%	0.44 ± 4%	0.14 ± 23%	1.11 ± 39%	1.53 ± 27%	0.66 ± 64%
Total OC (g C)	33.4 ± 16%	5.0 ± 44%	-20.8 ± 23%	238.7 ± 7%	12.7 ± 21%	7.6 ± 103%
DOC	11.4 ± 3%	2.9 ± 69%	5.3 ± 31%	225.2 ± 11%	8.5 ± 24%	7.0 ± 47%
FPOC	9.0 ± 54%	2.2 ± 33%	-23.2 ± 19%	0.8 ± 1697%	0.5 ± 336%	-2.9 ± 236%
CPOC	13.1 ± 15%	-0.1 ± 319%	-2.9 ± 10%	12.7 ± 64%	3.7 ± 9%	3.4 ± 60%
DO (g O ₂)	-23.9 ± 6%	-16.6 ± 8%	12.5 ± 15%	-217.0 ± 33%	-39.2 ± 6%	-16.8 ± 20%
free CO ₂ (g C)	19.6 ± 27%	11.7 ± 8%	1.4 ± 78%	176.8 ± 40%	13.7 ± 9%	11.6 ± 48%
Alkalinity (eq)	2.9 ± 31%	10.8 ± 38%	1.6 ± 9%	17.3 ± 18%	1.5 ± 9%	4.2 ± 100%
Si (g Si)	12.1 ± 6%	7.1 ± 9%	-0.3 ± 440%	34.7 ± 47%	8.5 ± 9%	6.9 ± 26%
Chla, total	-0.3 ± 4%	-0.1 ± 14%	-0.2 ± 19%	-0.7 ± 25%	-0.1 ± 13%	-0.2 ± 27%
FSS	119.3 ± 56%	43.5 ± 71%	-628.2 ± 12%	-15.1 ± 1990%	33.6 ± 110%	-107.9 ± 104%
CSS	111.6 ± 3%	-0.7 ± 576%	-11.6 ± 27%	122.6 ± 60%	36.2 ± 7%	33.9 ± 20%
O₂ demand (g O₂)	110.0 ± 13%	30.1 ± 17%	-72.2 ± 19%	731.3 ± 12%	67.0 ± 10%	33.7 ± 64%
DOM (OR=2.1)	23.9 ± 3%	6.1 ± 69%	11.1 ± 31%	473.0 ± 11%	17.8 ± 24%	14.7 ± 47%
FPOM (OR=2.9)	26.1 ± 54%	6.4 ± 33%	-67.3 ± 19%	2.3 ± 1697%	1.4 ± 336%	-8.3 ± 236%
CPOM (OR=2.4)	31.3 ± 15%	-0.4 ± 319%	-6.9 ± 10%	30.5 ± 64%	9.0 ± 9%	8.3 ± 60%
NH ₄ ⁺ (OR=4)	4.8 ± 6%	1.3 ± 40%	3.5 ± 4%	8.5 ± 130%	-0.4 ± 134%	2.3 ± 37%
DO	23.9 ± 6%	16.6 ± 8%	-12.5 ± 15%	217.0 ± 33%	39.2 ± 6%	16.8 ± 20%

MKC (Apr. 1-2, 2008) – a period of very low tide range in early spring before the marsh grass began to green up and actively grow – showed a very different pattern in net loads from all the other sampling periods (Tables 3-4). Most notable was that the marsh provided a strong sink for nitrate and all fine and coarse particulate fluxes (i.e. FSS, FPOC FPON, CSS, CPOC, CPON, and Chlorophyll a). These might be explainable because all of these species had much higher concentrations in the Murderkill River endmember than observed at any other time, perhaps due to a spring “flush”. An unexplainable result, on the other hand, is that our calculations from our own DO data show that the marsh was a source of DO to the Estuary. However, this result is not corroborated by the continuous dissolved oxygen data, collected at the same site by the US Geological Survey. Although there was a gap in the USGS DO data from 3-8 am on April 2, the other running 25-hour average anomalies from March 31 to April 3

were negative (i.e. a DO sink). Furthermore, during the storm-free period from March 24 to April 6, the four positive excursions in the running 25-hour average anomalies were small (i.e. about 10-20% of the typical negative anomaly) and short (1-6 hours). We cannot explain the reason for this discrepancy between the hourly sample-based data and the continuous data for the period.

Table 4. Net loads to the Murderkill Estuary from Webbs Marsh, in units of $\mu\text{mol}/\text{m}^2/\text{d}$ for better comparison of stoichiometry, otherwise similar to Table 3.

Mean Flux	MKA Jul Jul. 2007 $\mu\text{mol}/\text{m}^2/\text{d}$	MKB Oct Oct. 2007 $\mu\text{mol}/\text{m}^2/\text{d}$	MKC Apr Apr. 2008 $\mu\text{mol}/\text{m}^2/\text{d}$	MKD May May 2008 $\mu\text{mol}/\text{m}^2/\text{d}$	MKE Aug Aug. 2008 $\mu\text{mol}/\text{m}^2/\text{d}$	Average Excluding MKD $\mu\text{mol}/\text{m}^2/\text{d}$
Total N ($\mu\text{mol N}$)	1100 \pm 19%	101 \pm 187%	-720 \pm 41%	2652 \pm 44%	451 \pm 45%	233 \pm 195%
NO ₃ ⁻ + NO ₂ ⁻	78 \pm 13%	-11 \pm 92%	-456 \pm 28%	-919 \pm 19%	-36 \pm 14%	-106 \pm 123%
NH ₄ ⁺	233 \pm 6%	64 \pm 40%	169 \pm 4%	416 \pm 130%	-21 \pm 134%	111 \pm 37%
DON	812 \pm 19%	13 \pm 1438%	419 \pm 57%	3317 \pm 28%	390 \pm 49%	408 \pm 96%
FPON	-200 \pm 69%	40 \pm 72%	-808 \pm 13%	-348 \pm 103%	27 \pm 204%	-235 \pm 79%
CPON	177 \pm 15%	-5 \pm 140%	-44 \pm 14%	186 \pm 65%	91 \pm 6%	55 \pm 52%
Total P ($\mu\text{mol P}$)	55 \pm 16%	87 \pm 7%	20 \pm 23%	160 \pm 4%	223 \pm 3%	96 \pm 13%
PP, total	7 \pm 104%	3 \pm 114%	0 \pm 0%	51 \pm 56%	-2 \pm 164%	2 \pm 399%
PO ₄ ³⁻	51 \pm 13%	45 \pm 10%	8 \pm 19%	11 \pm 84%	90 \pm 15%	48 \pm 32%
TDP (PO ₄ +DOP)	47 \pm 9%	39 \pm 4%	12 \pm 23%	98 \pm 39%	135 \pm 27%	58 \pm 64%
Total OC ($\mu\text{mol C}$)	7635 \pm 16%	1138 \pm 44%	-4749 \pm 23%	54500 \pm 7%	2907 \pm 21%	1733 \pm 103%
DOC	2597 \pm 3%	667 \pm 69%	1207 \pm 31%	51419 \pm 11%	1940 \pm 24%	1603 \pm 47%
FPOC	2057 \pm 54%	505 \pm 33%	-5297 \pm 19%	184 \pm 1697%	114 \pm 336%	-655 \pm 236%
CPOC	2981 \pm 15%	-34 \pm 319%	-659 \pm 10%	2898 \pm 64%	854 \pm 9%	785 \pm 60%
DO ($\mu\text{mol O}_2$)	-2046 \pm 6%	-1420 \pm 8%	1073 \pm 15%	-18580 \pm 33%	-3357 \pm 6%	-1438 \pm 20%
free CO ₂ ($\mu\text{mol C}$)	4469 \pm 27%	2665 \pm 8%	312 \pm 78%	40375 \pm 40%	3126 \pm 9%	2643 \pm 48%
Alkalinity (μeq)	7826 \pm 31%	29458 \pm 38%	4299 \pm 9%	47530 \pm 18%	4101 \pm 9%	11421 \pm 100%
Si ($\mu\text{mol Si}$)	1185 \pm 6%	693 \pm 9%	-28 \pm 440%	3384 \pm 47%	833 \pm 9%	671 \pm 26%
O2 demand ($\mu\text{mol O}_2$)	11799 \pm 13%	2941 \pm 17%	-7940 \pm 19%	77145 \pm 12%	6541 \pm 10%	3335 \pm 64%
DOM (OR=1.05)	2727 \pm 3%	700 \pm 69%	1268 \pm 31%	53990 \pm 11%	2037 \pm 24%	1683 \pm 47%
FPOM (OR=1.45)	2983 \pm 54%	732 \pm 33%	-7681 \pm 19%	266 \pm 1697%	165 \pm 336%	-950 \pm 236%
CPOM (OR=1.2)	3577 \pm 15%	-41 \pm 319%	-791 \pm 10%	3477 \pm 64%	1024 \pm 9%	943 \pm 60%
NH ₄ ⁺ (OR=2)	465 \pm 6%	129 \pm 40%	338 \pm 4%	832 \pm 130%	-42 \pm 134%	222 \pm 37%
DO	2046 \pm 6%	1420 \pm 8%	-1073 \pm 15%	18580 \pm 33%	3357 \pm 6%	1438 \pm 20%

MKD captured the large water fluxes draining the marsh following the “Mother’s Day Storm” of 2008, showing marsh fluxes that were about an order of magnitude larger than any of the other 4 sampling periods (Tables 3 and 4). Of particular note were the very high DOC, DON and DO fluxes that dominated total average oxygen demand fluxes to the Murderkill of 731 $\text{gO}_2/\text{m}^2/\text{y}$ (\pm 12%) or 77,100 $\mu\text{mol}/\text{m}^2/\text{d}$. For this reason we excluded MKD net load values from our averages. However, the MKD results provide an exceptionally valuable insight into the role of storm events in driving large fluxes to and from salt marshes in the Murderkill Estuary.

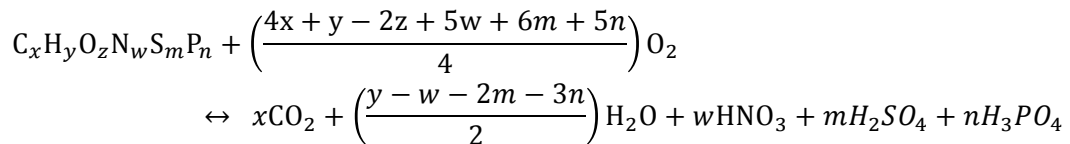
MKE (Aug. 2008) exhibited net loads that were similar in pattern and magnitude to MKA (Tables 3-4). DO deficit fluxes in MKE were larger and CPOM fluxes were smaller than MKA.

Total average oxygen demand fluxes to the Murderkill Estuary for this 2-day period were 67 gO₂/m²/y (±10%) or 6,540 μmol/m²/d.

Inspection of net load values and their errors (Table 3 and 4) demonstrate the effectiveness of our novel approach to quantifying fluxes using concentration anomalies to conservative mixing. However, our results also highlight the intrinsic natural temporal variability in net loads in these highly dynamic salt marsh systems that are not only driven by ever-changing tides but also by episodic storm and wind events (Wong et al., 2009; Dzwonkowski et al., 2013). Therefore, temporal extrapolation of these net loads for use in modeling studies is not straightforward. Ideally, the concentrations of all biogeochemically active species would be measured continuously over a 1-2 year study period so that we could calculate daily net loads. However, DO was the only bioactive species measured continuously at Webbs Marsh over this 18-month study period. These data and a statistical analysis of DOC loads from Webbs Marsh to the Murderkill Estuary will be the subject of a separate report. For all other species we can only provide average values (Tables 3 and 4). Even with the exclusion of MKD, these average values contain much larger uncertainties than was typically observed for each 2-day sampling period suggesting that physical and other processes, not considered in this report, control nutrient, carbon, and particle exchange between Murderkill salt marshes and the Murderkill Estuary. Despite this, our study provides for the first time quantitative estimates of net loads to and from a salt marsh.

4.7 Recommended oxidation ratios for the respiration of organic matter.

Previously used conversion factors to estimate carbon mineralization from oxygen consumption have been used inconsistently by different research communities and have not taken into consideration the latest data on the topic. Most textbooks write out the reversible photosynthesis/respiration reaction as: CO₂ + H₂O ← → CH₂O + O₂, in which all carbon is fixed to carbohydrates and the molar oxidative ratio (R = O₂/CO₂) is 1. Redfield et al. (1963) expanded this reaction stoichiometry to include nitrogen and phosphorus for marine systems where these nutrients are supplied as or mineralized to nitrate (NO₃⁻) and phosphate (PO₄⁻³) respectively. Since then many studies have elucidated how OR depends both on the oxidation state of the fixed/respired organic matter and on the oxidation state of involved inorganic nitrogen species and to a lesser extent sulfur species (Anderson, 1995; Hedges et al., 2002; Masiello et al., 2008). Thus, complete oxidation of organic matter with an elemental composition of C_xH_yO_zN_wS_mP_n follows the following reaction stoichiometry:



Where the average oxidation state (C_{ox}) of carbon in the organic matter is given as:

$$C_{ox} = \frac{2z - y + 3w + 2m - 5n}{x}$$

This presumes that organic N predominately has a +3 oxidation state (i.e. amide), that organic S predominately has a +2 oxidation state (i.e. thiol, sulfide), that natural sulfate esters with a -6 oxidation state contribute negligibly, and that organic P has a -5 oxidation state (i.e. phosphate ester). A simplified formulation of oxidation ratio can be attained by rearranging the ratio of the stoichiometric coefficients of O₂ and CO₂ to the following forms that depend on the oxidation state of the inorganic nitrogen:

$$\text{nitrate: } OR = 1 - \frac{C_{ox}}{4} + \frac{2w}{x} + \frac{2m}{x}$$

$$N_2: OR = 1 - \frac{C_{ox}}{4} + \frac{3w}{4x} + \frac{2m}{x}$$

$$\text{Ammonia: } OR = 1 - \frac{C_{ox}}{4} + \frac{2m}{x}$$

Organic sulfur and phosphate contribute minimally to natural organic matter, and ignoring their terms in these calculations introduces only small errors.

Many studies provide the respiratory quotient (RQ), which is the inverse of the oxidation or respiration ratio (i.e. RQ = 1/OR = ΔCO₂/ΔO₂).

Despite this knowledge, many aquatic studies (e.g. Webster et al., 1999) use a molar oxidation ratio of 1 (i.e. the Biology 101 textbook value). Yet other aquatic studies (i.e. Williams and del Giorgio, 2005) take the physiological perspective that organisms excrete reduced nitrogen (i.e. urea or NH₃) and therefore ignore that in heterotrophic oxic aquatic systems, inorganic nitrogen is typically rapidly oxidized to nitrate. On the other hand, in terrestrial systems nitrogen is often supplied as N₂ or NH₄⁺ depending on the importance of nitrogen fixation or fertilization. These net community transformations of nitrogen need to be explicitly considered in calculating OR. For example, the OR of a typical protein can be 1.04 or 1.56 depending on whether the organic nitrogen is ultimately transformed to ammonium or nitrate. For this study, we assume that all reduced nitrogen species (both organic N and NH₄⁺) are oxidized to nitrate, as is observed in nearly all aquatic systems. Last, recent studies have refined the elemental ratios of fixed/respired organic matter to better reflect actual biochemical compositions of marine plankton (Anderson, 1995; Hedges et al., 2002) and soil organic matter (Baldock et al., 2004; Hockaday et al., 2009). Due consideration of all of these factors contributing to net OR is critical for accurate assessments of organic carbon quality and use.

We can use this background to inform our choices of OR values for our study of organic matter loads from Webbs Marsh to the Murderkill Estuary, and also for OR values for sediment oxygen demand within the Murderkill Estuary. Although we did not measure organic oxygen or hydrogen values, our direct measurements of C:N ratios provide a strong direct constraint on OR values. Furthermore, C:N along with isotopic composition can further guide our choice of values based on values from the literature. Published studies where C:H:O:N are all measured found that from molar OR = 0.95 from wetland DOC (Gu et al., 1995), plant tissue and soil organic matter have OR ~ 1.2 (Hockaday et al., 2009), marine plankton have OR ~ 1.4 (Hedges

et al., 2002), and proteins have $OR = 1.55$ and above depending on nitrogen and sulfur content. For this study, we have therefore selected molar OR values of: 1.05 mol/mol for DOM because of its high C:N ratios (15-30); 1.2 mol/mol for CPOM because of its moderate C:N (12-18) and isotopic signatures of marsh grasses; and 1.45 mol/mol for FPOM because of its low C:N (6.5-11) that require a very high protein content. We recommended these same values be used in Murderkill modeling studies.

4.8 Implications for the Murderkill Estuary

- Salt marshes are most often a significant source of dissolved nutrients and dissolved organic matter to the Murderkill Estuary and, through the Estuary, to Delaware Bay. The fluxes of dissolved nutrients result from the remineralization of organic matter in marsh sediments and are apparently released from the sediments at the end of ebb tide through lateral discharge to marsh channels. Although most of the water exiting the marsh retains the chemistry of the water that initially flooded into the marsh on the previous flood tide, the release of the products of sediment remineralization at the end of ebb tides leads to a periodic and distinctive change in composition that can be used to calculate significant dissolved nutrient and carbon loads from the marsh.
- Based on C/N ratios and C and N isotopic compositions there are two distinctive populations of organic particles that are exchanged during periods of peak flow between the Murderkill salt marshes and the Estuary itself. Fine particles – with C/N = 6.5 to 10.3, $\delta^{13}C = -26\text{‰}$ to -20‰ , and $\delta^{15}N = 5\text{‰}$ to 10‰ – represent contributions from both marine phytoplankton and soil organic matter and are carried both into and out of the Marsh. Coarse particles have compositions similar to the DOM – with C/N = 11.1 to 21.1, and $\delta^{13}C = -22\text{‰}$ to -18‰ , and $\delta^{15}N = 5\text{‰}$ to 10‰ – and represent contributions from vascular plant detritus and are dominantly exported from the marsh.
- The well-mixed nature of the lower Murderkill Estuary, and the focus of nutrient loads from the Murderkill marshes to the Murderkill Estuary during the short period of time toward the end of ebb tide, permits the use of a novel method for the determination of dissolved nutrient fluxes from the marshes to the Estuary. This method, based on the deviation of the non-conservative compositions of ebb tidal waters from the well-mixed and conservative flood tidal waters permits the determination of nutrient loads from the Murderkill marshes to the Murderkill Estuary with much greater precision than simple summed load techniques. This method also focuses on ebb-tidal fluxes only, thus eliminating problems in load determination during periods of water imbalance. The greater precision of the experimentally determined loads means that models, based on these loads, will be better constrained than using the summed load techniques.
- The depletion of dissolved O_2 as estuarine waters reside in salt marshes represents an O_2 -deficit load that can be considered an export of biogeochemical oxygen demand to the Murderkill Estuary. It reduces O_2 concentrations in the Murderkill below saturation levels as effectively as marsh export of reduced compounds (DOM, NH_4^+ , and POM). In fact, these O_2 -deficit loads contributed 22% to 58% of the total oxygen demand (excluding MKC) delivered from Webbs Marsh. Thus, proper inclusion of O_2 -deficit loads

is required to use hydrodynamic/water quality models for realistic ecosystem management.

- Loads of particulate and dissolved nutrients, carbon and DO deficit loads are extremely variable on multiple time scales. Tidal influences are obvious on the hourly time scales and variability in tidal forcing controlling tidal velocities, discharge, and loads over longer time scales (daily, weekly, monthly, and seasonal) are clearly important controls as well. Sub-tidal flows, such as those generated by offshore winds and storms, also influence average loads at daily, weekly, monthly, seasonal and annual time scales.

5 Acknowledgements:

Funding for this work was provided through a cooperative agreement between the Kent County Board of Public Works (Hans Medlarz, County Engineer) and the Delaware Department of Natural Resources and Environmental Control (DNREC; Hassan Mirsajadi, Project Director). We acknowledge assistance and support from colleagues at the US Geological Survey (Anthony Tallman, Dover, DE) and the Murderkill Working Group (Andrew Thuman, Hydroqual, Inc.; Thomas E. McKenna, Delaware Geological Survey; Jonathan Sharp, University of Delaware; Xia Xie, DNREC; John Schneider, DNREC; David Wolanski, DNREC; Ben Pressley, DNREC; David McQuaide, DNREC, Allison Rogerson, DNREC; David Velinsky, Drexel University).

This project could not have been accomplished without the skilled help of a number of volunteers who worked odd shifts both night and day in order to collect and analyze the necessary samples. Among these are:

- University of Delaware: Yaohong Zhang, Skye Schmidt, Emily Maung, Jill (Brown) Bourque, Ryan Dale, Brian Dzwonkowski, Joe Scudlark, Ellen McGinnis, Tracy Eelsey-Quirk, Mia Steinberg, Jen (Halcheck) Dann, Kara Winslow, Julie Anderson, and Adam Pimenta, and Joe Scudlark.
- Stroud Water Research Center: Sarah (Geleski) Damiano, Mike Gentile, Vivian Williams, Rebecca Lyne, Alessa Wood, Jennifer Matkov, Amanda Conover, Linda Carter and Hahn Ngyuen.
- Maella Dréan (Institute Universitaire de Technologie, Perpignan, France)
- Jennifer Volk (DNREC)

This report is dedicated to Dr. Kent S. Price (1936-2012) who fostered this project and many others designed to bring good and creative science to bear on the management of the Murderkill Watershed and Estuary and other similar ecosystems in Delaware.

6 Citations

- Anderson, L. A. 1995. On the hydrogen and oxygen content of marine phytoplankton. *Deep Sea Research Part I: Oceanographic Research Papers*, 42(9): 1675-1680.
- Andres, A.S. 2004. RI66 Ground-Water Recharge Potential Mapping in Kent and Sussex Counties, Delaware. *Delaware Geological Survey Report of Investigation*.
- Aufdenkampe, A. K., Hedges, J. I., Richey, J. E., Krusche, A. V., & Llerena, C. A. 2001. Sorptive fractionation of dissolved organic nitrogen and amino acids onto fine sediments within the Amazon Basin. *Limnology and Oceanography*, 46(8): 1921-1935.
- Aufdenkampe, A. K., Mayorga, E., Hedges, J. I., Llerena, C., Quay, P. D., Gudeman, J., Krusche, A.V., & Richey, J. E. 2007. Organic matter in the Peruvian headwaters of the Amazon: Compositional evolution from the Andes to the lowland Amazon mainstem. *Organic Geochemistry*, 38(3): 337-364.
- Aufdenkampe, A. K., Mayorga, E., Raymond, P. A., Melack, J. M., Doney, S. C., Alin, S. R., Aalto, R.E., & Yoo, K. 2011. Riverine coupling of biogeochemical cycles between land, oceans, and atmosphere. *Frontiers in Ecology and the Environment*, 9(1): 53-60.
- Baldock, J. A., Masiello, C. A., Gelinas, Y., & Hedges, J. I. 2004. Cycling and composition of organic matter in terrestrial and marine ecosystems. *Marine Chemistry*, 92(1): 39-64.
- Coplen, T. B., Brand, W. A., Gehre, M., Gröning, M., Meijer, H. A., Toman, B., & Verkouteren, R. M. 2006. New guidelines for $\delta^{13}\text{C}$ measurements. *Analytical Chemistry*, 78(7): 2439-2441.
- De Michele, E. 1972. The effects of conservative substances on the Murderkill River. Report to the Department of Natural Resources and Environmental Control, Dover, Delaware, 101 p.
- deWitt, P., and Daiber, F.C. 1974. The hydrography of the Murderkill Estuary, Delaware. *Chesapeake Science*, 15: 84-95.
- DNREC, 2001. Technical Analysis for Murderkill River TMDLs. Delaware Department of Natural Resources and Environmental Control, Dover DE. pp. 113.
- DNREC, 2004. Technical Analysis for Amendment of the 2001 Total Maximum Daily Loads (TMDLs) for the Murderkill River Watershed. Delaware Department of Natural Resources and Environmental Control, Dover, DE. pp. 122.
- DNREC, 2005. Final Regulation Amending the Maximum Daily Loads for the Murderkill River Watershed. Delaware Department of Natural Resources and Environmental Control, Dover DE. pp. 27.
- DNREC, 2006. TMDLs for Bacteria for the Murderkill River Watershed, Delaware. Delaware Department of Natural Resources and Environmental Control, Dover DE. pp. 1.
- Dzwonkowski, B., Wong, K. -C. & Ullman, W. J. 2011. Episodic Shifts in Sea Level and Velocity Characteristics of a Salt Marsh Tidal Creek of the Murderkill Estuary, DE. (Report submitted to Kent County Board of Public Works, 9 June 2011)

- Dzwonkowski, B., Wong, K. -C. & Ullman, W. J. 2013. Water level and velocity characteristics of a salt marsh channel in the Murderkill Estuary, Delaware. (*Journal of Coastal Research*). doi:<http://dx.doi.org/10.2112/JCOASTRES-D-12-00161.1>
- Fofonoff, N. P., & Millard, R. C. 1983. Algorithms for computation of fundamental properties of seawater. UNESCO Technical Papers in Marine Science. No. 44. pp. 53.
- Gardner, L. R. 2005. A modeling study of the dynamics of pore water seepage from intertidal marsh sediments, *Estuarine Coastal Shelf Sci.*, 62: 691– 698.
- Gu, B., Schmitt, J., Chen, Z., Liang, L., & McCarthy, J. F. 1995. Adsorption and desorption of different organic matter fractions on iron oxide. *Geochimica et Cosmochimica Acta*, 59(2): 219-229.
- Hays, R.L. 2009. Vegetation Patterns and Nutrient Cycling in Delaware Bay Salt Marshes: Great Marsh (Lewes) and Webbs Marsh (South Bowers), Delaware. Ph.D. dissertation, College of Earth, Ocean, and Environment, University of Delaware.
- Hedges, J. I., Baldock, J. A., Gélinas, Y., Lee, C., Peterson, M. L., & Wakeham, S. G. 2002. The biochemical and elemental compositions of marine plankton: A NMR perspective. *Marine Chemistry*, 78: 47-63.
- Hockaday, W. C., Masiello, C. A., Randerson, J. T., Smernik, R. J., Baldock, J. A., Chadwick, O. A., & Harden, J. W. 2009. Measurement of soil carbon oxidation state and oxidative ratio by ¹³C nuclear magnetic resonance. *Journal of Geophysical Research*, 114(G2): G02014.
- Howes, B. L., & Goehring, D. D. 1994. Porewater drainage and dissolved organic carbon and nutrient losses through the intertidal creekbanks of a New England salt marsh. *Marine Ecology Progress Series*, 114: 289-301.
- Lane, S. L., Flanagan, S., & Wilde, F. D. 2003. Selection of Equipment for Water Sampling (ver. 2.0). pp. 101. In: F. D. Wilde, D. B. Radtke, J. Gibs, R. T. Iwatsubo, S. L. Lane et al., eds. *U.S. Geological Survey Techniques of Water-Resources Investigations, book 9, National Field Manual for the Collection of Water-Quality Data, chap. A2*, Vol. 9. U.S. Geological Survey.
- Masiello, C. A., Gallagher, M. E., Randerson, J. T., Deco, R. M., & Chadwick, O. A. 2008. Evaluating two experimental approaches for measuring ecosystem carbon oxidation state and oxidative ratio. *Journal of Geophysical Research: Biogeosciences (2005–2012)*, 113(G3).
- Millero, F.J. 1979. The thermodynamics of the carbonate system in seawater. *Geochimica et Cosmochimica Acta*, 43: 1651-1661.
- Millero, F.J., 1995. Thermodynamics of the carbon dioxide system in the oceans. *Geochimica et Cosmochimica Acta*, 59:661-677.
- NRCS. 2007. Rapid Watershed Assessment: Broadkill-Smyrna Watershed, Delaware. Natural Resources Conservation Service, US Department of Agriculture, Beltsville, MD. pp. 37.

- Osburn, C. L., & St-Jean, G. 2007. The use of wet chemical oxidation with high-amplification isotope ratio mass spectrometry (WCO-IRMS) to measure stable isotope values of dissolved organic carbon in seawater. *Limnology & Oceanography: Methods*, 5: 296-308.
- Redfield, A. C., Ketchum, B. H., & Richards, F. A. 1963. The influence of organisms on the composition of sea-water. p. 26-77. In: M. N. Hill [ed.], *The Sea: Ideas and Observations on Progress in the Study of the Seas*, Vol. 2. Wiley.
- Richardson, D. C., Kaplan, L. A., Newbold, J. D., & Aufdenkampe, A. K. 2009. Temporal dynamics of seston: A recurring nighttime peak and seasonal shifts in composition in a stream ecosystem. *Limnology and Oceanography*, 54(1): 344-354.
- Richardson, D. C., Newbold, J. D., Aufdenkampe, A. K., Taylor, P. G., & Kaplan, L. A. 2013. Measuring heterotrophic respiration rates of suspended particulate organic carbon from stream ecosystems. *Limnology and Oceanography Methods*, 11: 247-261.
- St-Jean, G. 2003. Automated quantitative and isotopic (^{13}C) analysis of dissolved inorganic carbon and dissolved organic carbon in continuous-flow using a total organic carbon analyser. *Rapid Communications in Mass Spectrometry*, 17(5), 419-428.
- Webster, J. R., Benfield, E. F., Ehrman, T. P., Schaeffer, M. A., Tank, J. L., Hutchens, J. J. & D'Angelo, D. J. 1999. What happens to allochthonous material that falls into streams? A synthesis of new and published information from Coweeta. *Freshwater Biology*, 41: 687-705.
- Williams, P. J. & del Giorgio P. A. 2005. Respiration in aquatic ecosystems: history and background. In: P.A. del Giorgio, and P.J. Williams (Eds.), *Respiration in Aquatic Ecosystems*. New York, New York: Oxford University Press, pp. 1-17.
- Wilson, A. M. & Gardner, L.R. 2006. Tidally driven groundwater flow and solute exchange in a marsh: Numerical simulations. *Water Resources Research*, 42:W01405. doi:10.1029/2005WR004302.
- Wong, K.-C., Dzwonkowski, B. & Ullman, W. J. 2009. The temporal and spatial variability of sea level and volume flux in the Murderkill Estuary. *Estuarine, Coastal, and Shelf Science* 84: 440-446.
- Zeebe, R. E. & Wolf-Gladrow, D. 2001. *CO₂ in Seawater: Equilibrium, Kinetics, and Isotopes*. Elsevier, Amsterdam. pp. 346.

7 Appendices:

Data tables on CD attached to report, with images of tables below.

Abreviation	Units	Source	Description
Sample DateTime (EDT)			Date and Time of sample collection in local daylight time (Eastern Daylight Time)
Sample Code			Unique Sample Name (XXY-NN (MK = "Murderkill;" Y= A (July07), B (Oct07) C (Apr08), D (May08); E (Aug08); F (Aug08); N or NN= sequential sample number
pH		UD	Hydrogen ion activity
T (°C)	°C	UD	Temperature in °C
Salinity	Salinity	UD	Salinity (unitless, but essentially equivalent to ppt or ‰ -- parts per thousand)
O ₂ %sat	%	UD	Dissolved O ₂ concentration expressed as a percent of the concentration of O ₂ at equilibrium with the atmosphere in water at the specified salinity and temperature
O ₂ (µM)	µM	UD	Dissolved O ₂ concentration in units of µM
Chla Total (µg/L)	µg/L	UD	Total Chlorophyll a concentration, measured in unsieved samples
Chla Sieved	µg/L	UD	Chlorophyll a concentration, measured in samples that pass through a 63µm sieve
PP Total (µM)	µM	UD	Particulate phosphorus measured in unsieved samples
PP Sieved (µM)	µM	UD	Particulate phosphorus measured in samples that pass through a 63µm sieve
NO ₃ ⁻ (µM)	µM	UD	Dissolved Nitrate (NO ₃ ⁻) + Nitrite (NO ₂ ⁻) concentration
NH ₄ ⁺ (µM)	µM	UD	Dissolved Ammonium (NH ₄ ⁺) concentration
DON (µM)	µM	UD	Dissolved Organic Nitrogen concentrations
PO ₄ ³⁻ (µM)	µM	UD	Dissolved Soluble Reactive Phosphorus (SRP, ΣPO ₄ , or orthophosphate)
TDP (µM)	µM	UD	Total dissolved phosphorus concentration
DOP (µM)	µM	UD	Dissolved organic phosphorus
Si (µM)	µM	UD	Dissolved silicate
Alkalinity (µeq/L)	µeq/L	SWRC	Total alkalinity of a filtered (0.45 µm)
DOC (µM)	µM	SWRC	Dissolved organic carbon
DOC/N	mol/mol	SWRC/UD	Molar C/N ratio in dissolved organic matter, caculated from both SWRC and UD data
DOC-13 (‰)	‰	SWRC	δ ¹³ C of dissolved organic carbon (DOC)
FSS (mg/L)	mg/L	SWRC	Fine particle (suspended solids) concentration (particles that pass through a 63µm sieve)
%OC FSS	%	SWRC	Weight percent organic carbon of FSS
FPOC (µM)	µM	SWRC	Carbon in fine particles (particles that pass through a 63µm sieve) per liter of water sampled
FPON (µM)	µM	SWRC	Nitrogen in fine particles (particles that pass through a 63µm sieve) per liter of water sampled
FPOC/N (mol/mol)	mol/mol	SWRC	Molar C/N ratio in fine particles (particles retained by a 63µm sieve)
FPOC-13 (‰)	‰	SWRC	δ ¹³ C in fine particles (particles that pass through a 63µm sieve)
FPON-15 (‰)	‰	SWRC	δ ¹⁵ N in fine particles (particles that pass through a 63µm sieve)
CSS (mg/L)	mg/L	SWRC	Coarse particle (suspended solids) concentration (retained by a 63µm sieve)
%OC CSS	%	SWRC	Weight percent organic carbon of CSS
CPOC (µM)	µM	SWRC	Carbon in coarse particles (particles retained by a 63µm sieve) per liter of water sampled
CPON (µM)	µM	SWRC	Nitrogen in coarse particles (particles retained by a 63µm sieve) per liter of water sampled
CPOC/N (mol/mol)	mol/mol	SWRC	Molar C/N ratio in coarse particles (particles passing through a 63µm sieve)
CPOC-13 (‰)	‰	SWRC	δ ¹³ C in coarse particles (particles retained by a 63µm sieve)
CPON-15 (‰)	‰	SWRC	δ ¹⁵ N in coarse particles (particles retained by a 63µm sieve)
DIC (µM)	µM	SWRC	Dissolved inorganic carbon
DIC-13 (‰)	‰	SWRC	δ ¹³ C of dissolved inorganic carbon (DIC)
Equilibrium pCO ₂ (ppm)	ppm	Derived	Partial pressure of CO ₂ at equilibrium with the free CO ₂ * (CO ₂ (aq) + H ₂ CO ₃ ^o (aq)) present in the water sample, derived from pH and Alkalinity
Free CO ₂ [CO ₂ *] (µM)	µM	Derived	(CO ₂ (aq) + H ₂ CO ₃ ^o (aq)) present in the water sample, derived from pH and Alkalinity
Gauge Date & Time (EST)		USGS	Date and Time of instataneous USGS data closest in time to sample collection, in local standard time (Eastern Standard Time)
Gage Ht (ft)	ft	USGS	USGS gauge height at bridge outlet to Webb's Marsh (01484084)
Velocity (ft/s)	ft/s	USGS	USGS mean water velocity at bridge outlet to Webb's Marsh (01484084)
Discharge (CFS)	ft ³ /s	USGS	USGS calculated disharge at bridge outlet to Webb's Marsh (01484084)
Date & Time (EST)		Derived	Data and Time of hour corresponding to houly smoothed estimated parameters by B. Dzwonkowski et al. (2013)
Discharge (m ³ /s)	m ³ /s	Derived	Houly smoothed estimated discharge, caculated from USGS instaneous data by B. Dzwonkowski et al. (2013)
Salinity (psu)	psu	Derived	Houly smoothed estimated salinity caculated from USGS instaneous data by B. Dzwonkowski et al. (2013)

